WFPS:TME-81-031
NOVEMBER 1981
UC-20d

MASTER

WFPS-TME--81-031

DE82 007195

NEUTRON ATTENUATION IN THE LASER DUCTS OF AN INERTIAL-CONFINEMENT FUSION REACTOR

FRANK AUGUSTINE, Jr.
RENSSELAER POLYTECHNIC INSTITUTE
NUCLEAR ENGINEERING DEPARTMENT

COOPERATIVE GRADUATE EDUCTION PROGRAM IN FUSION TECHNOLOGY
ADMINISTERED FOR THE U.S. DEPARTMENT OF ENERGY
BY THE WESTINGHOUSE ELECTRIC CORPORATION
CONTRACT DE-AC02-77ET51010

MGW

DISCLAIMER

ACKNOWLEDGEMENT

This work was performed for the Office of Fusion Energy, U.S. Department of Energy, under Contract DE-AC02-77ET51010, "Cooperative Graduate Education Program in Fusion Technology." Reproduction, translation, publication, use and disposal, in whole or in part, by or for the United States Government is permitted.

Thanks are due to Dr. Pat Soran at the Los Alamos National Laboratory and especially to Dr. Lawrence Green and the other personnel at the Fusion Power Systems Department at Westinghouse for their help and advice.

Printed in the United States of America
Available From
National Technical Information Service
U.S. Department of Commerce
5285 Port Royal Road
Springfield VA 22161

NTIS Price Codes
Printed Copy: A04
Microfiche Copy: A01

WFPS:TME-81-031
NOVEMBER 1981
UC-20d

NEUTRON ATTENUATION IN THE LASER DUCTS OF AN INERTIAL CONFINEMENT FUSION REACTOR

PREPARED BY:

Frank Augustine, Jr.
Graduate Student Program Participant
Rensselaer Polytechnic Institute

REVIEWED BY:

Gordon Gibson, Manager
Nuclear and Plasma Engineering

APPROVED BY:

T. C. Varljen, Manager
Engineering

ABSTRACT

This report deals with the problem of neutron streaming through the laser beam ducts of an inertial confinement fusion power plant. The neutron flux through these ducts must be attenuated by a factor of 10^{12} to meet radiological safety limits. The problem is dealt with by using mirrors to bend the path of the laser beam while cutting off a line of sight path for neutrons. The Monte Carlo Code MCNP was used to analyze the two mirror SOLASE design, which only attenuated the neutron flux by a factor of 10^{3}. The Westinghouse design, initially assuming four mirrors, attenuated the neutron flux by 10^{4} per mirror bend, and hence only three mirror bends were needed. Further studies also revealed that the large length/diameter ratio of the ducts and the thinner mirror design were crucial to the large attenuation. It may also be possible to develop a two mirror system, at 10^{6} attenuation per mirror bend, utilizing improvements such as point cross overs, a second flux trap, and acute column-to-column angles. Further studies are needed to check this possibility.

CONTENTS

Page

LIST OF TABLES iv

LIST OF FIGURES v

ABSTRACT vii

1. INTRODUCTION 1

2. DISCUSSION OF CALCULATIONS AND CALCULATIONAL MODELS 6

2.1 MONTE CARLO TECHNIQUES AND COMPUTER CODES 6
2.2 DESCRIPTION OF MCNP 8
2.3 COMPUTER MODELS 10

2.3.1 SOLASE BLANKET MODEL 10
2.3.2 SOLASE LD/NA SYSTEM MODELS 12
2.3.3 WESTINGHOUSE LD/NA SYSTEM MODELS 12
2.3.4 EFFECTS OF SOURCE MODEL ON LD/NA STUDIES 15

3. RESULTS AND DISCUSSION 17

3.1 SIMPLIFIED SOLASE BLANKET 17
3.2 SOLASE LD/NA SYSTEM 17
3.3 WESTINGHOUSE LD/NA SYSTEM 20

4. CONCLUSIONS 27

LITERATURE CITED 32

APPENDIX A 33

DATA ON SOLASE BLANKET AND LD/NA SYSTEM 34
DATA ON WESTINGHOUSE BLANKET AND LD/NA SYSTEM 43

APPENDIX B 55

SHORTCOMINGS OF MCNP 56
ERROR MESSAGES 57
TIPS ON USAGE OF MCNP 58
A LISTING OF TEST PROGRAMS AND COMPUTER PLOTS 64

LIST OF TABLES

		Page
Table I	Monte Carlo Codes	7
Table II	MCNP	9
Table III	Results of SOLASE Blanket Analysis	18
Table IV	Results of SOLASE LD/NA System Analysis	19
Table V	Results of SOLASE LD/NA System (Without Mirrors) Analysis	21
Table VI	Results of Westinghouse LD/NA Systems Analysis	22
Table VII	Results of Westinghouse LD/NA System Analysis (Without Flux Trap)	23
Table VIII	Results of Westinghouse LD/NA System Analysis (Without Mirrors)	24
Table IX	Results of Westinghouse LD/NA System Analysis	26

LIST OF FIGURES

		Page
Figure 1	University of Wisconsin SOLASE Mirror-Beam Duct System Configuration	4
Figure 2	Suggested Mirror-Beam Duct Configuration Changes for Increased Attenuation from SOLASE Study	5
Figure 3	Simplified SOLASE Blanket Model	11
Figure 4	Comparison of SOLASE Mirror Beam-Duct Configuration with MCNP Calculational Model	13
Figure 5	Calculational Model of Westinghouse Blanket and Mirror Beam-Duct Configuration	14
Figure 6	Mirror Beam Duct System with Acute Column to Column Angles	28
Figure 7	Differential Elastic Scattering Cross Section for Aluminum, Center of Mass System	30
Figure 8	Beam Cross Over Systems	31

PART 1

INTRODUCTION

An important consideration in the design of inertial confinement fusion (ICF) power plants based on laser drivers is the problem of neutron streaming through the reaction chamber penetrations and along the laser beam ducts. This large streaming flux can have adverse economic implications for an ICF power plant. The Class A structure housing the reaction chamber must include all the elements of the optical train along which the dose rates are in excess of radiological limits. The cost of the structure (which is resistant to earthquake, flood, hurricane, tornado, and other possible disasters) is a major part of the plant costs, so it is essential that its size be minimized. If we assume beam entry from the laser building to be through quartz windows, it is necessary that the radiation field at the windows be reduced to levels which permit normal access by radiation workers during reactor operation. Estimates of neutron dose rates indicate that for a 3000 MW(t) reactor, a neutron attenuation of about 10^{12} is needed to achieve this level. It is also important that this condition be satisfied with the fewest possible number of elements in the laser duct/neutron attenuation system. Both direct costs and maintenance procedures are impacted by the number of elements.

The basic problem then, is to maximize neutron attenuation through the laser ducts while minimizing overall size. The purpose of this study is to propose and analyze possible solutions to this problem.

The approach most commonly used in this problem is to use mirrors to bend the path of the laser beam several times so that no line of sight path for neutrons exists. Because of the limitations in laser energy density

incident on the mirrors to about 5 J/cm^2 during a laser pulse, large surface area mirrors are required. This leads to large penetrations and duct diameters, conditions which exacerbate neutron streaming. The strong forward peaking of secondary neutrons produced in high energy non-elastic reactions further compounds the problem. Still, as judged by cost and technical feasibility, this approach is best. Some of the other problems of this approach are:

- Heating and degradation of the optical properties of the last mirror, which is exposed directly to the source of the neutron flux.
- Optical restrictions on the last mirror which both focuses and reflects the laser beam.
- Neutron reflection along the ducts.

The first problem, heating and degradation of the last mirror, is usually dealt with by using a gas or liquid cooled metal mirror. Chemically, metals stand up best under neutron irradiation and are far easier to cool than non-metals which generally have a low thermal conductivity. Because of its light weight, aluminum is usually chosen as the structural material, with a thin copper coating serving as the reflecting surface. The second problem, optical restrictions, has been analyzed by Howard[1]. He concludes that the last mirror must bend the laser by 90° or more if it is to focus the laser beam onto the pellet properly. The third problem depends on the specific mirror and duct geometry, and can vary considerably in severity from system to system.

A recent attempt to deal with the laser duct/neutron attenuation problem was in the SOLASE study, a comprehensive attempt to determine the costs, parameters and overall design of an inertial confinement reactor. The

study was performed under the Fusion Research Program at the Nuclear Engineering Department of the University of Wisconsin.

The SOLASE duct system (Fig. 1) uses 2 aluminum mirrors, each of which bend the laser beam 90°, in each of 12 beam ducts. In each beam duct, the last mirror is water cooled. Periodic replacement and easy access to the last mirror was an assumed requirement, and this significantly affected duct/mirror geometry. Minimizing costs in materials and construction was also considered.

The SOLASE design allows for access of the last mirror by using a liquid shield behind the mirror. This can be pumped out when access is needed. Materials costs are minimized by using concrete shielding. Construction cost is minimized by keeping the size relatively small and the distance between mirrors short.

Subsequent Monte Carlo analysis revealed however, that after two bends, the flux was only attenuated by a factor of 10^3, resulting in a flux of 10^9 n/cm^2 sec, or a neutron dose rate of 10^6 mr/hr. This is a totally unacceptable solution. Several factors, including the use of the thick water cooled mirror and the short distance between mirrors were believed to be responsible. Some improvements were suggested (Fig. 2) including beam crossovers, flux traps, annular beam illumination, mechanical beam chopping devices for reactors with low repetition rates, thinner gas cooled mirrors and longer inter mirror distances. Some of these suggested improvements are utilized in this report, while others have been left for further investigation.

In conjunction with this study, a Westinghouse laser duct/neutron attenuation was designed and analyzed. The Westinghouse blanket is more complex, but the laser duct/neutron attenuation (LD/NA) system is simpler than the SOLASE design. For comparison purposes, and as a check on the calculational methods, the SOLASE LD/NA system was reanalyzed.

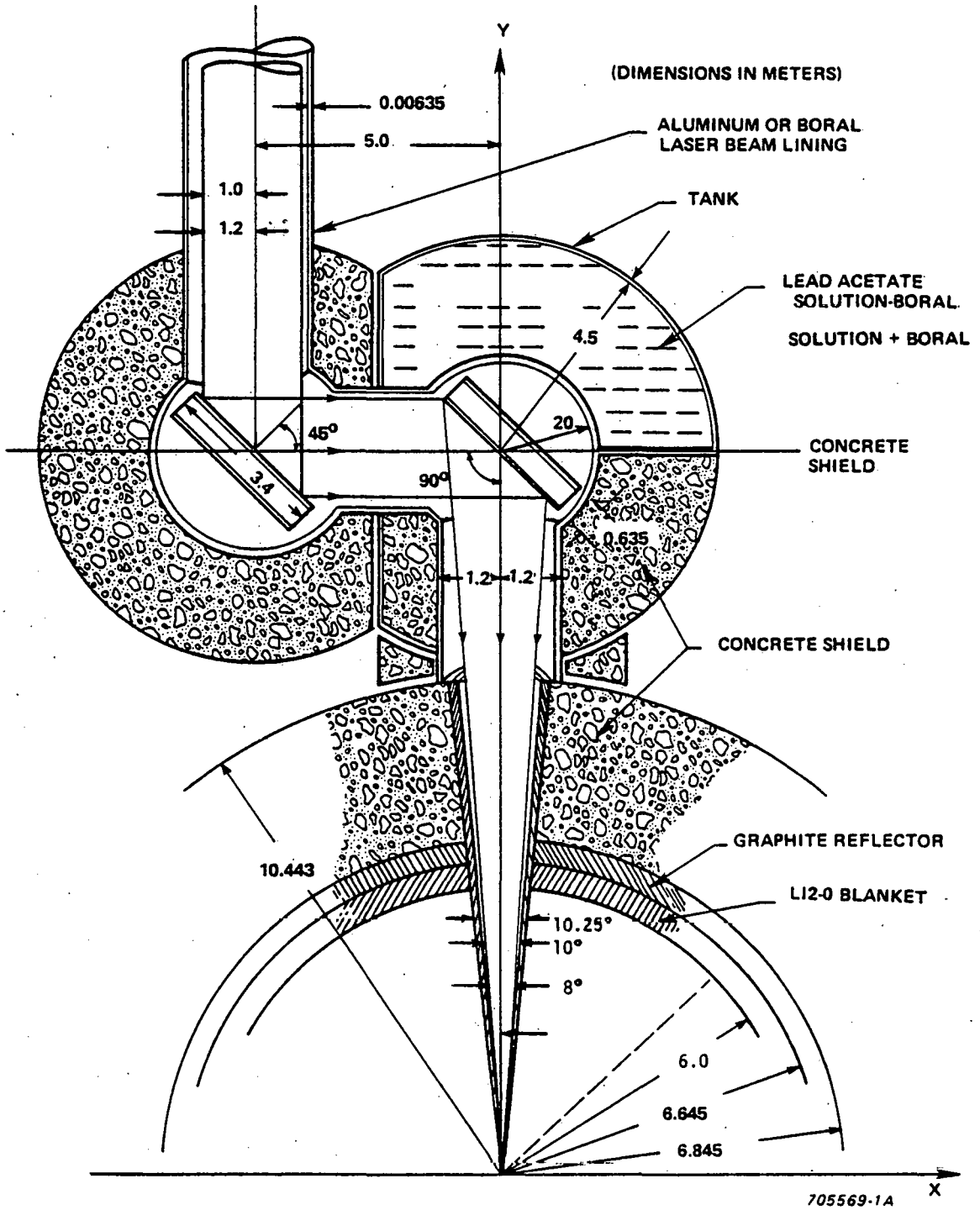

Figure 1. University of Wisconsin SOLASE Mirror-Beam Duct System Configuration.

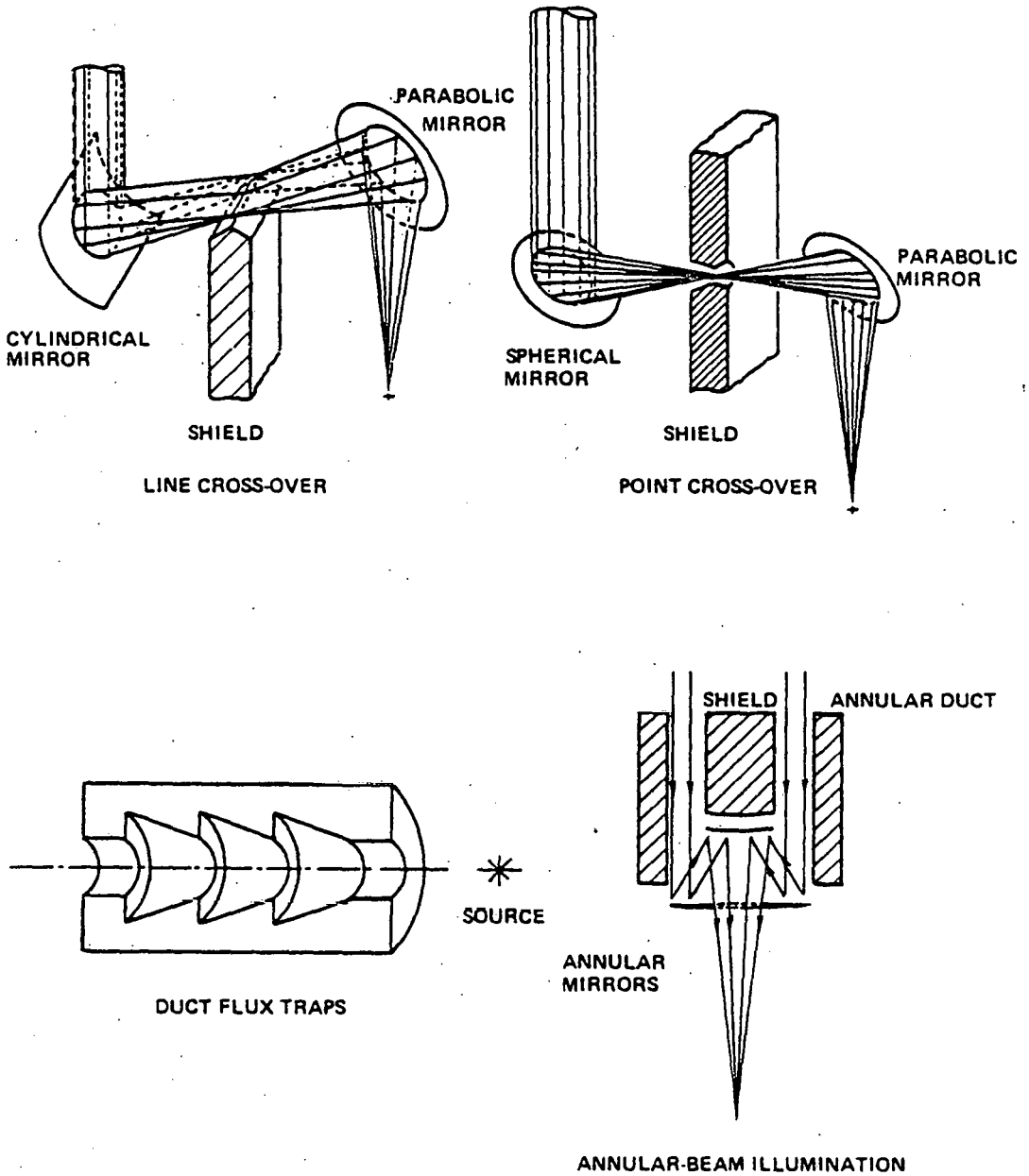

Figure 2. Suggested Mirror-Beam Duct Configuration Changes for Increased Attenuation from SOLASE Study.

PART 2

DISCUSSION OF CALCULATIONS AND CALCULATIONAL MODELS

2.1 Monte Carlo Techniques and Computer Codes

The need for a 3-dimensional analysis of the LD/NA system is obvious. Moreover Monte Carlo is the only tractable calculational method. Any deterministic code (if one with the necessary geometric capabilities were available) would probably require longer run times. In addition, Monte Carlo codes are versatile and can be used just about wherever neutronics calculations are needed. Codes are available for heterogeneous and homogeneous LWR lattice type problems, two dimensional problems, fast reactor problems, criticality problems, and problems with unusually complex geometries. Heating rates, multiplication factors, neutron albedos, and breeding ratios can be computed by these codes as well as fluxes, currents, simple neutron counting, and angular energy, and/or time distributions of neutrons. For this problem adequate statistics, utilizing standard variance reduction techniques, were obtained in run times of five minutes or less. Some Monte Carlo codes are listed in Table I.

Most Monte Carlo codes can be divided into four aspects: geometric capabilities, cross sectional capabilities, variance reduction techniques and calculational capabilities.

For this problem, the code MCNP (Monte Carlo code for Neutrons and Photons) was chosen. MCNP is a non-lattice, general purpose code with a great variety of variance reduction schemes, wide calculational capabilities, and a flexible geometric capability, all of which were important in a LD/NA system problem.

TABLE I

MONTE CARLO CODES

CODE NAME	PROBLEM TYPE
KENO	Lattice, Criticality Problems
MORSE	General Purpose Including Lattices
MCNP	General Purpose, No Lattices Continuous Energy
VIM	Continuous Energy, Lattices Fast Reactor Calculations Some Thermal Neutron Scattering Capability
TRIPOLI	General Purpose, No Lattices More Accurate than MORSE
TRIMARAN	Criticality Studies, No Lattices
SAM-CE	General Purpose Including Lattices

2.2 Description of MCNP

MCNP has four main subprograms (Table 2). Subprograms IMCN, XACT and MCRUN are encountered in that order during the normal running of the program, assuming the input file is free of errors. PLOT is used when the inputted geometry is to be plotted on a Cathode Ray Tube (CRT) terminal.

The geometry in MCNP is constructed by specifying equations of surfaces in a three dimensional cartesian coordinate system. Regions of space can have a positive sense with respect to a surface (containing points for which $f(x, y, z) > o$, $f(x, y, z) = o$ being the equation of the surface), or a negative sense. Regions are specified in terms of the intersection or union of positive or negative senses of surfaces and are composed of a homogeneous mixture of any elements the user wishes to specify. Surfaces may be one or two degree surfaces or toroidal type fourth degree surfaces.

MCNP uses continuous energy data from any one of several cross section libraries, most notably, the ENDF/B library. All reactions available in the cross section libraries can be used in MCNP calculations, including gamma production cross sections for Monte Carlo calculations of photon distributions. More than one library may be used if cross section data is incomplete. Temperature cannot be specified and is assumed to be absolute zero (cross sections are not Doppler broadened) for the cross section file available.

MCNP has a wide variety of variance reduction techniques, which can be used to increase accuracy, reduce computer time, or both. Some of the techniques available are russian roulette, geometry splitting, energy, time, and statistical weight cutoffs, exponential transforms, energy splitting, and source biasing. Several of these techniques were used in the analysis of LD/NA systems.

TABLE II

MNCP

IMCN	-	CHECKS INPUT FILE FOR ERRORS COMPUTES VOLUMES AND SURFACE AREAS COMPUTES MATERIAL PARAMETERS TABULATES INPUT DATA PROCESSES PROBLEM GEOMETRY
XACT	-	TAKES CROSS SECTION DATA FROM SPECIFIED LIBRARY
PLOT	-	PLOTS ANY CROSS SECTION OF THE THREE-DIMENSIONAL GEOMETRY CAN ENLARGE SECTIONS OF GEOMETRY OR ROTATE THEM, PRODUCING NEW INPUT DATA IF NECESSARY
MCRUN	-	RUNS PARTICLE HISTORIES

MCNP has many useful calculational capabilities. The code can compute currents, surface fluxes, average flux in a volume, flux at a point, energy deposition in a volume, and several other distributions and reaction rates. Several of these features were used to compare the calculations to computations by other neutronics codes.

2.3 Computer Models

To model a LD/NA system, it is generally unnecessary to model all the mirrors and ducts neutronically. Except for the last mirror, which must be cooled, the other mirrors and the geometry of the duct system which houses them all is nearly identical. If four mirrors are assumed, at 10^3 attenuation per mirror bend, a 10^6 attenuation occurs after two bends. Verification of a 10^{12} attenuation would be quite expensive using Monte Carlo, and hence two-mirror models are chosen for the Monte Carlo simulation. The attenuation attainable for two mirrors, squared, is assumed to be the attenuation attainable for four.

2.3.1 SOLASE Blanket Model

The first models simulated in this study were simple, to gain experience in constructing and running the input file for MCNP. These models did not contain mirrors, but, nevertheless, were valuable in comparing MCNP with calculations from other neutronics codes. The first such model (Figure 3) simulated a simplified SOLASE blanket. This blanket was significantly different neutronically than the actual case. The actual case used concrete rather than lead and a graphite grid in the Li_2O blanket. This lead to a significantly higher tritium breeding ratio than in the actual blanket, but not unexpected as the simplified blanket is a nearly ideal case. The source in the simplified case was a 14 MeV mono-energetic source as in the SOLASE

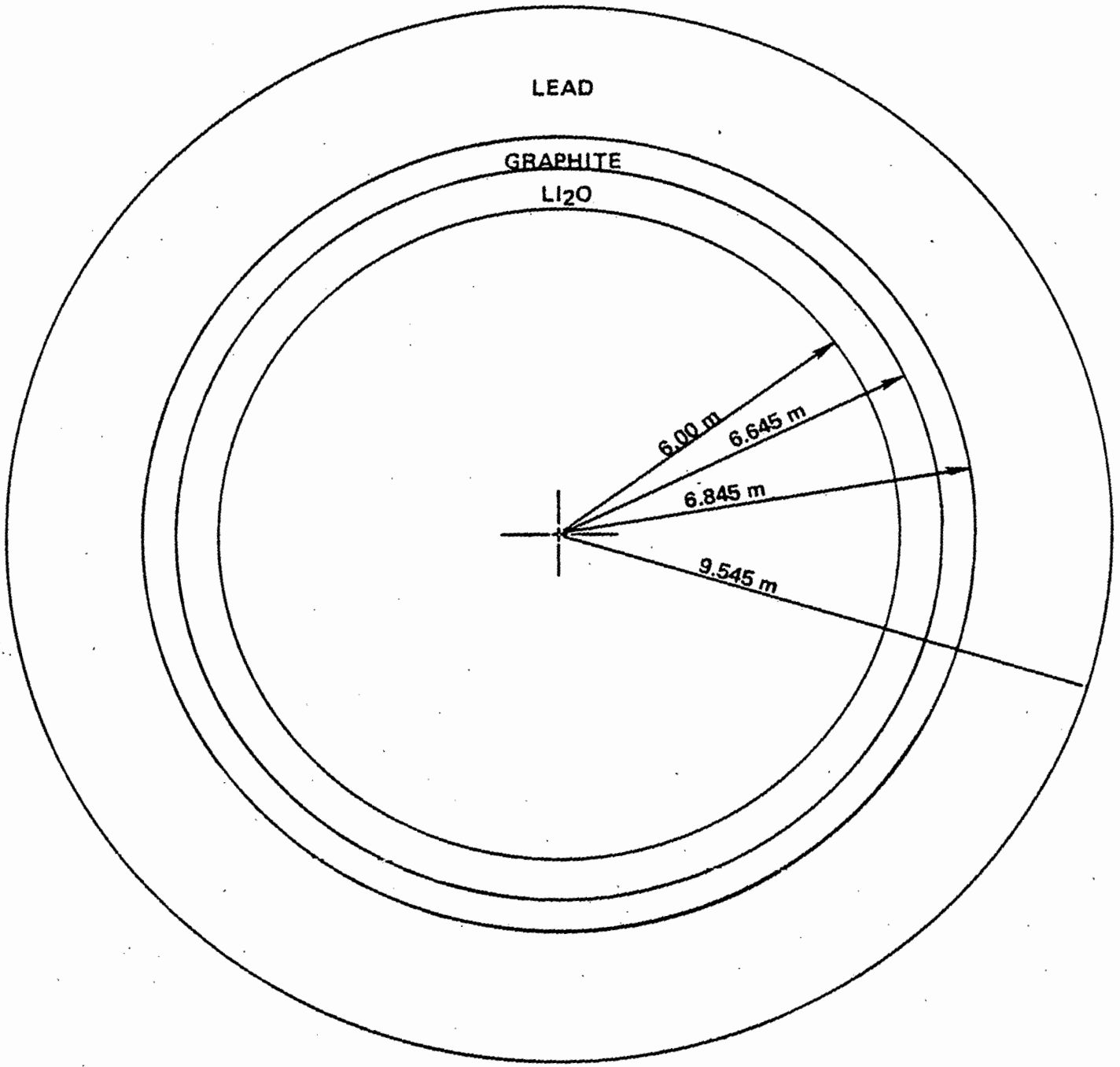

Figure 3. Simplified SOLASE Blanket Model.

study, for comparison with the SOLASE results.

2.3.2 SOLASE LD/NA System Models

After analysis of several intermediate models (discussed in Appendix B) the SOLASE LD/NA system was modeled, with some small differences (Fig. 4 a,b). These differences included: 1) the use of aluminum plating on the inner surfaces of the duct in the SOLASE study model but not in the MCNP model; 2) the slightly increased diameter of concrete and liquid shielding in the MCNP model; 3) slight differences in the geometry of the ducts and; 4) the use of the full spherical blanket in the MCNP rather than a conical segment with a reflecting boundary.

Of the differences, the first one was probably the most important in giving too low an attenuation. In addition, MORSE was used in the SOLASE LD/NA system study rather than MCNP (MORSE is a general purpose code containing extremely versatile geometric capabilities including lattices, and great flexibility in adapting to different computer systems). Both models used a monoenergetic 14 MeV source.

2.3.3 Westinghouse LD/NA System Models

After a few more intermediate models were studied, the Westinghouse blanket and LD/NA system was modeled (Fig. 5). Several improvements over the SOLASE LD/NA system were made in this design: 1) the distance from the chamber center to the first mirror was increased to 30 m rather than 15 m; 2) the distance between mirrors was increased from 5 m to 20 m; 3) the mirrors were thinned from 63.5 cm to 32.0 cm; 4) the last mirror was gas cooled rather than water cooled; 5) the diameter of the duct was reduced to 1 m; 6) the beam dump behind mirror A was restructured as to be a flux trap .

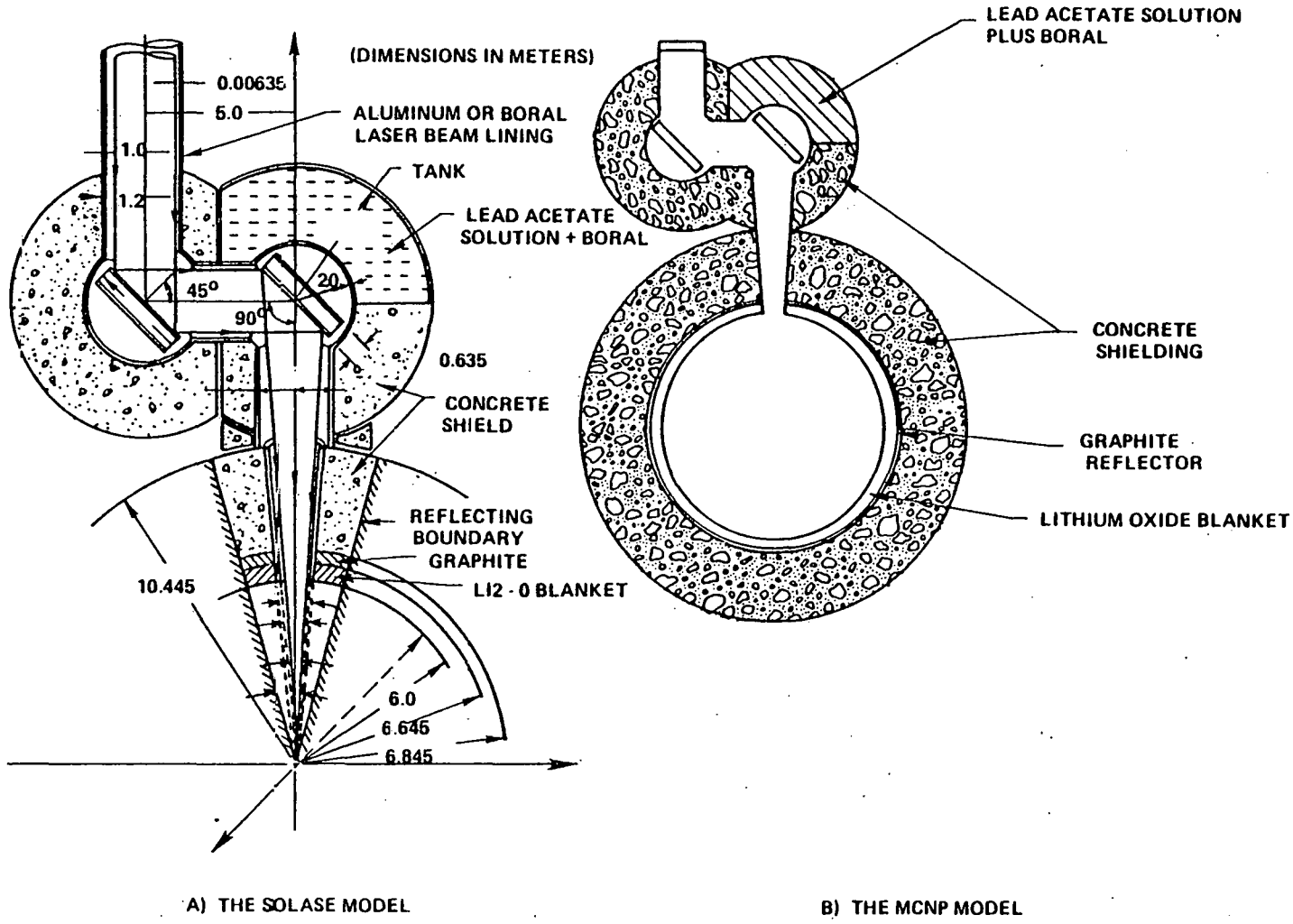

Figure 4. Comparison of SOLASE Mirror Beam-Duct Configuration with MCNP Calculational Model.

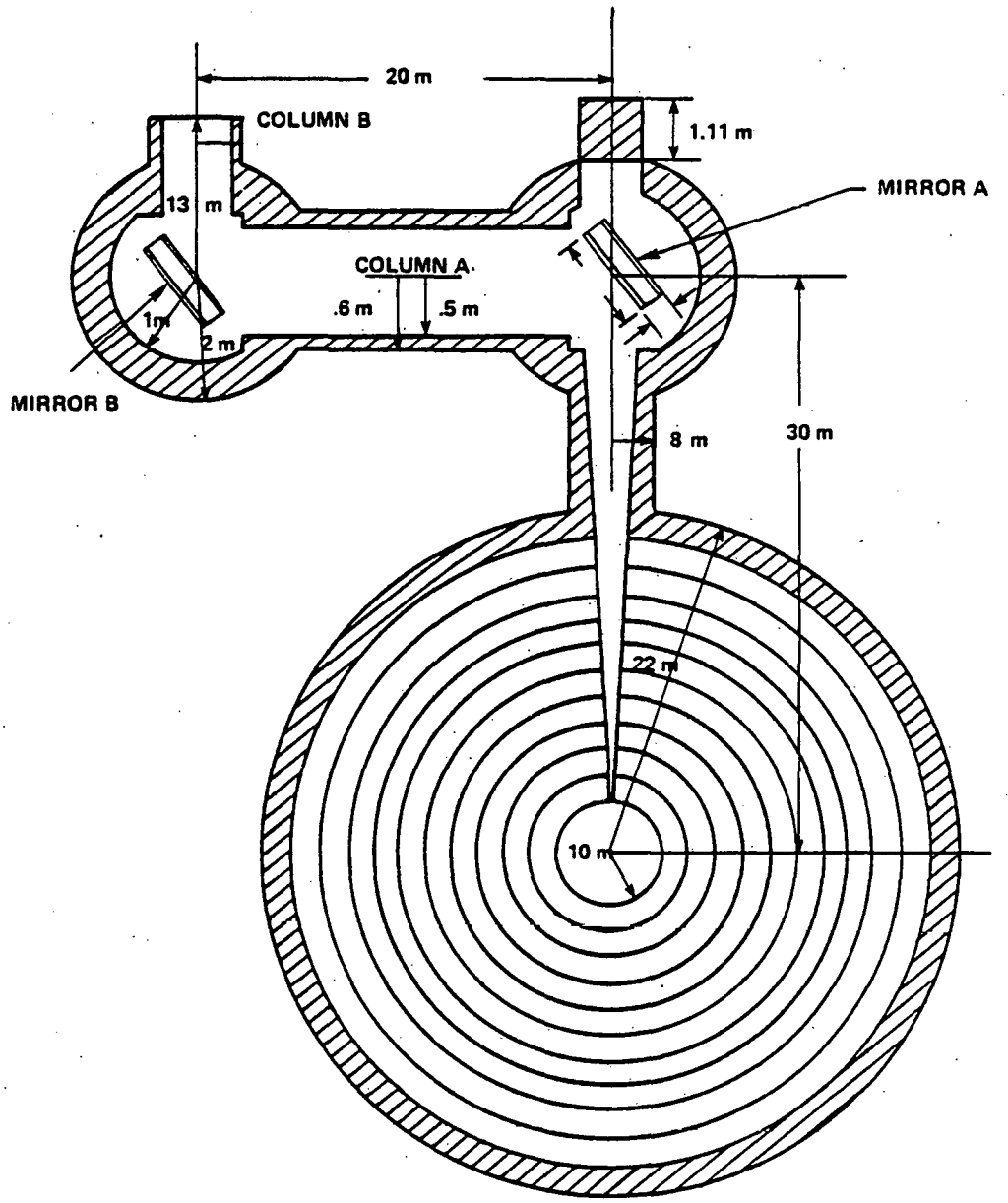

Figure 5. Calculational Model of Westinghouse Blanket and Mirror Beam-Duct Configuration.

Since the specifications for the Westinghouse LD/NA system were developed in conjunction with this study, the MCNP model constitutes an accurate description of its design. The blanket representation was only approximate. However, blanket neutronics has very little effect on the attenuation properties of the LD/NA system. Therefore, the MCNP results provide a good estimate of the attenuation characteristics of the Westinghouse design.

The flux trap behind mirror A serves three functions. First, it absorbs the pellet neutron energy transmitted through the mirror (about 50 MW). This requires that the shielding behind the mirror be actively cooled, and the geometry of a flux trap makes this less difficult. Secondly, the flux trap provides for convenient access to the mirror. This is important since mirror A will require frequent replacement. Finally, overall attenuation is improved by reducing the number of neutrons scattered towards the next mirror.

One further difference which should be mentioned is the variety of instruments, cooling equipment, and other devices in the actual system. This probably makes little difference overall neutronically, although it may be difficult to adequately shield such equipment from radiation damage.

2.3.4 Effects of Source Model on LD/NA Studies

The use of a 14 MeV monoenergetic source model was essential to LD/NA system calculations. For blanket calculations, a homogeneous volume 14 MeV source was used inside a compressed deuterium tritium pellet to accurately simulate a pellet source, except in the SOLASE blanket. For a LD/NA system, however, a cone source was needed to save computer run time. Even if a homogeneous volume source was started inside a conical segment of a pellet, any that scattered before leaving the pellet would probably go in the wrong direction and miss the cone ducts. Any that did not scatter would be 14 MeV

anyway, so a conical segment homogeneous volume source really made no difference, except that particles missing the cone duct would use up computer time.

It is difficult to predict what effect the use of a 14 MeV monoenergetic source model will have on the overall attenuation of a LD/NA system. Scattering cross sections are roughly constant in this range, absorption cross sections decrease, and other reactions (such as neutron multiplication, alpha or proton production) increase. Based on experience with other shielding systems, it is expected that a 14 MeV monoenergetic source will be slightly conservative is estimating the overall attenuation.

The size of the source cone used was larger than the size of the duct in the SOLASE LD/NA system studies. A cone source larger than the duct accurately simulated an isotropic source, allowing particles to scatter into the duct from the blanket. Studies of the system revealed, however, that very few particles that scattered into the duct from the blanket reached the mirror chamber, and that most of the particles that reached this chamber had been emitted from the source in that direction. This justified reducing the source cone size to the size of the duct, and this was done in most of the Westinghouse LD/NA system studies. When the attenuation after two mirrors was studied, however, different results emerged. Although the number of particles reaching the mirror chamber was the same, the angular distribution of those particles was different leading to improved attenuation when a source cone was used that was larger than the duct. A source cone equaling the duct size was used to save computer time, but it must be recognized that this produces a conservative result.

PART 3

RESULTS AND DISCUSSION

3.1 Simplified SOLASE Blanket

The results of the simplified SOLASE blanket study are in Table III, along with the results for the actual SOLASE blanket. As expected, the tritium breeding ratio is much higher for the simplified case. A more accurate SOLASE blanket (and the Westinghouse blanket) was run using MCNP. Both models used a 14 MeV isotropic monoenergetic source for comparison with the SOLASE study results. See Appendix A for details.

3.2 SOLASE LD/NA System

The results of the analysis of the SOLASE LD/NA system using MCNP are compared with the MORSE results in Table IV. The fluxes and heating rates are difficult to compare because the MORSE values did not included standard deviations. From the paper which these results were obtained from, it can be inferred that the error is much larger than in this study.

Attenuation is far lower than was assumed in the costing phase of the SOLASE study. One of the reasons for the low attenuation is the relatively low length to diameter ratio of the column between mirrors. It is really not a column but simply a hole joining the two mirror chambers. Any neutron reflected off mirror A or the shielding surrounding mirror A has a significant chance of hitting mirror B because of the low L/D ratio.

Although it is obvious that increasing the L/D ratio would improve the attenuation, other measures to improve attenuation are not obvious. It is uncertain whether neutrons are reflected mostly by the mirrors (in which case the mirror design should be improved) or by the shielding surrounding the

TABLE III

RESULTS OF SOLASE BLANKET ANALYSIS

		SIMPLIFIED BLANKET		COMPLEX BLANKET	
TRITIUM BREEDING RATIO	Lithium 6	.9016		.797	
	Lithium 7	.5711		.498	
	Total	1.4727		1.295	
		n	γ	n	γ
ENERGY DEPOSITION (MeV/Source Neutron)	Lithium Oxide	13.591	1.640	12.670	1.865
	Graphite	.008	.024	.123	.224
	Lead	.000	.207	.002	.262
	Total	13.599	1.871	12.795	2.351
	Grand Total	15.470		15.146	
	Energy Multiplication	1.105		1.082	
	Neutron Multiplication	1.064		1.040	

TABLE IV

RESULTS OF SOLASE LD/NA SYSTEM ANALYSIS

LOCATION	FLUXES ($n/cm^2/s$) MORSE	MCNP
Front Plate of Mirror A	4.73E13	2.797 ± 0.022E13
Front Plate of Mirror B	3.37E12	7.259 ± 0.594E11
Inside of Quartz Window	6.11E10	8.351 ± 3.14E10

MIRROR A	HEATING RATES (watts/cm^3, kilowatts) MORSE (n only)	MCNP (n)	MCNP (γ)
Front Plate	1.44 , 332.8	1.60 , 369.8	0.343 , 79.3
Honeycomb	0.31 , 164.4	0.034, 180.3	0.010 , 53.0
Backplate	0.87 , 201.1	0.87 , 201.1	0.273 , 63.1

ATTENUATION

(Particles in Cone/Particles Hitting Quartz Window)

MORSE: 769 MCNP: 563± 212

mirrors (in which case shielding geometry should be improved). In order to measure the relative albedoes of the mirror and the chamber shielding geometry, the input file for the SOLASE LD/NA system was modified so that the mirrors were removed. Running this input file produced the results in Table V.

Removal of the mirrors made a threefold difference in the overall attenuation. From comparison of the square roots of the attenuations (which is a rough calculation of the average attenuation per bend) with and without the mirrors, the mirror and shielding geometry can be judged to be about equally important in reflection of neutrons, so both the mirror design and the shielding geometry need improvement. It should be emphasized, however, that this result may not hold if the L/D ratio is significantly changed.

3.3 Westinghouse LD/NA System

The results of the analysis of the Westinghouse LD/NA system are given in Table VI. Attenuation (for two mirrors) has improved by a factor of 10^6. A great part of this improvement is due to the increased L/D ratio. The mirror design is also better as evidenced by the heating of the Westinghouse mirror A which is approximately a hundred times cooler than in the SOLASE design. Some of this difference is due to the smaller (by a factor of 27) solid angle of the Westinghouse duct. The thinness of the mirror then accounts for an approximately fourfold reduction in heating.

Because the shielding geometry still needed improvement, a flux trap was included in the design. In studies of the Westinghouse LD/NA system without the flux trap (Table VII), the attenuation was reduced only a factor of about two leading to the conclusion that the mirrors are much more important in neutron reflection in the Westinghouse LD/NA system than in the SOLASE LD/NA system. To confirm this, a case was run without the mirrors. The results are in Table VIII, and greatly reinforce the conclusion that the

TABLE V

RESULTS OF SOLASE LD/NA SYSTEM (WITHOUT MIRRORS) ANALYSIS

LOCATION	FLUXES ($n/cm^2/sec$)
RIGHT END OF HORIZONTAL COLUMN	1.719 ± .086 E12
LEFT END OF HORIZONTAL COLUMN	6.04 ± .451 E11
INSIDE OF QUARTZ WINDOW	2.803 ± 570 E10

ATTENUATION

(Particles in cone/particles hitting quartz window)

1677 ± 341

vs

563 ± 212 with mirrors

TABLE VI

RESULTS OF WESTINGHOUSE LD/NA SYSTEM ANALYSIS

Flux at Beginning of Horizontal Column	3.096 ± 0.06 E11 $n/cm^2/s$
Flux at End of Horizontal Column	5.729 ± 2.675 E8 $n/cm^2/s$
Flux at End of Vertical Column	7.066 ± 5.000 E3
Energy Deposition in Front Plate, Mirror A (n,γ)	5.07 kW, 905 W
Energy Deposition in Honeycomb, Mirror A (n,γ)	3.81 kW, 547 W
Energy Deposition in Backplate, Mirror A (n,γ)	3.19 kW, 656 W
Energy Deposition in Beam Dump (n,γ)	80.7 kW, 23.2 kW
Attenuations (Source Particles/Particles Reaching End of Vertical Column)	5.612 ± 3.971 E8

TABLE VII

RESULTS OF WESTINGHOUSE LD/NA SYSTEM ANALYSIS
(Without flux trap)

FLUX AT BEGINNING OF HORIZONTAL COLUMN	4.653 ± .121 E11
FLUX AT END OF HORIZONTAL COLUMN	7.004 ± 4.363 E8
FLUX AT END OF VERTICAL COLUMN	1.493 ± 1.056 E4

ATTENUATION

2.656 ± 1.878 E8

TABLE VIII

RESULTS OF WESTINGHOUSE LD/NA SYSTEM ANALYSIS
(Without Mirrors)

FLUX AT BEGINNING OF HORIZONTAL COLUMN	1.0348 ± .0031 E11	$n/cm^2/s$
FLUX AT END OF HORIZONTAL COLUMN	< 2.982 E6	$n/cm^2/s$
FLUX AT END OF VERTICAL COLUMN	< 7.456 E3	$n/cm^2/s$

ATTENUATION

> 9.454 E7

Out of 94,544,000 particles, none reached Mirror B.
Hence, attenuation around the first bend is approximately 10^8.

mirrors are very important in the Westinghouse LD/NA design, as the attenuation increases some four orders of magnitude per bend.

In order to gain a rough idea of the effect of the increased L/D ratio, a case was run with a 10 m separation between mirrors rather than a 20 m separation. The results (Table IX) show that the attenuation decreases by a factor of 25. To summarize then, in both the Westinghouse and SOLASE design the relative importance of the mirrors and the shielding geometry concerning neutron reflection was determined. In the SOLASE design, which utilized a small L/D ratio (2) the removal of the mirrors improved attenuation by a factor of 3 but in the Westinghouse design, which utilized an L/D ratio ten times larger, the removal of the mirrors improved attenuation by a factor of 10^4 (per mirror). The relatively small change (a factor of about 2) in attenuation that the removal of the flux trap made confirmed that the increased L/D ratio increased the neutron albedo of the mirror relative to the shielding geometry. The importance of the L/D ratio itself in attenuation was demonstrated by reducing the L/D ratio to ten in the Westinghouse design which reduced attenuation by a factor of 25.

TABLE IX

RESULTS OF WESTINGHOUSE LD/NA SYSTEM ANALYSIS
(Ten meter separation between mirrors)

FLUX AT BEGINNING OF HORIZONTAL COLUMN	3.102 ± .079 E11	$n/cm^2/s$
FLUX AT END OF HORIZONTAL COLUMN	1.860 ± .528 E9	$n/cm^2/s$
FLUX AT END OF VERTICAL COLUMN	2.152 ± 1.521 E7	$n/cm^2/s$

ATTENUATION

(Source particles/particles at end of vertical column)

2.152 ± 1.521 E7

PART 4

CONCLUSIONS

The SOLASE design assumed (in the costing phase) that the two mirror LD/NA system would reduce the neutron flux by a factor of 10^{12}. When follow up studies revealed only a 10^3 attenuation, Westinghouse in its comprehensive ICF reactor study assumed a four mirror system, attenuating neutrons by 10^3 per bend.

The main conclusions of this study is that a LD/NA system can be built utilizing only three mirrors providing a 10^4 attenuation per bend. A system that does this need not have exceedingly complex geometries (such as annular beam illumination or duct flux traps) or expensive mirror materials to attenuate the neutron flux adequately.

The main reason for this large attenuation is the larger L/D ratio and the mirrors, which are better designed than those in the SOLASE study and are considerably more important due to the larger L/D ratio.

Several improvements were suggested during the course of the study, all aimed at the possibility of using two mirrors rather than three. This would require a 10^6 attenuation per bend. An attenuation between 10^4 and 10^6 per bend would still require a third mirror, and probably would not be worth the extra expense required to go beyond the 10^4 per bend attained in the Westinghouse LD/NA system, unless other problems were alleviated, as in the addition of the beam dump. Some of the suggestions are:

1) Acute column to column angles (Fig.6). This would reduce the size of the mirrors and increase neutron attenuation, since the differential scattering cross sections decreases past 90°. The angle chosen would be

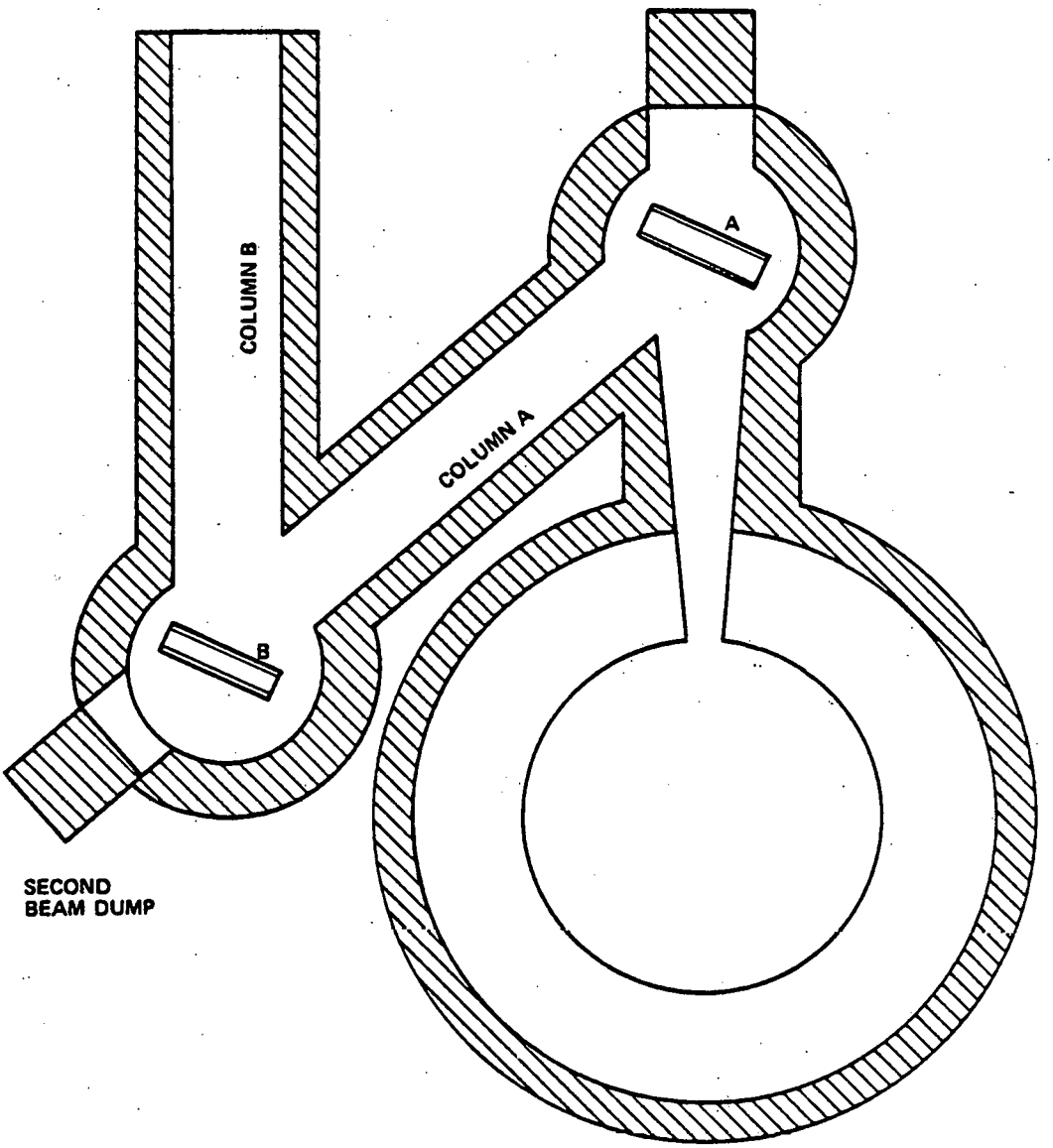

Figure 6. Mirror Beam Duct System with Acute Column to Column Angles.

the minimum of the differential scattering cross section curve. For aluminum (Fig. 7), this occurs at about 120° (at 14.1 MeV).

2) Adding a beam dump behind mirror B. This would increase attenuation by a factor of 2 or more, depending on the recession of the dump. If used with suggestion 1, it may be less effective because of the greater solid angle subtended by column B as viewed from the dump.

3) Beam crossover. There are two types, line crossovers and point crossovers (Fig. 8) of which point crossovers are more effective but more expensive.

4) Further research into thinning the mirror and using materials with lower scattering cross sections. The only limitation on the thickness of the mirror are structural limitations; the mirror must be strong enough to support its own weight and stiff enough to maintain the correct curvature. Additional limitations exist on the material for the mirror including: ease of adding a reflecting coating, high thermal conductivity, low density and low cost.

If all four of these suggestions were utilized, it may be possible to achieve a 10^6 attenuation/bend, in which case a two mirror LD/NA system could be envisioned. This is a topic for further investigation.

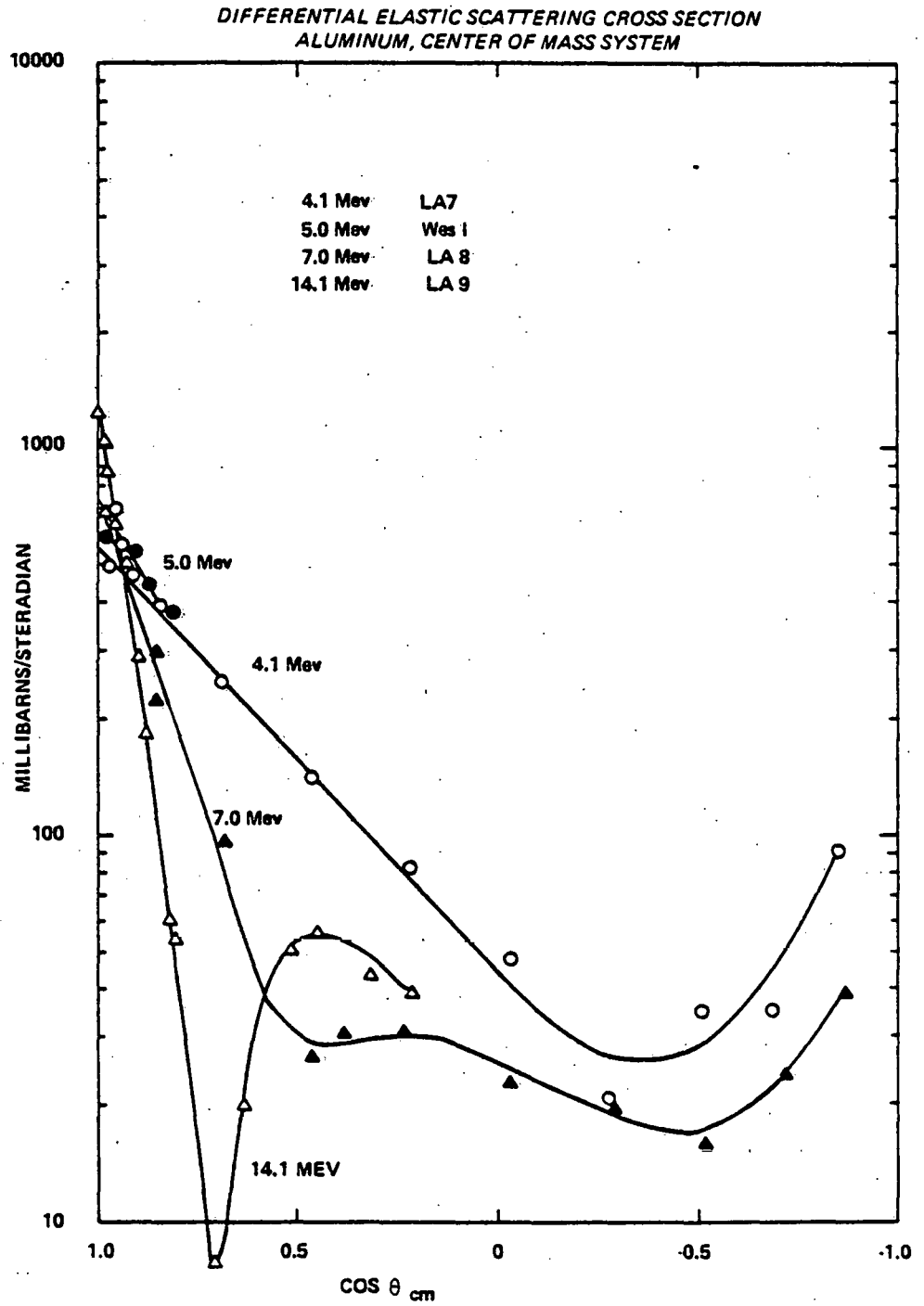

Figure 7. Differential Elastic Scattering Cross Section for Aluminum, Center of Mass System.

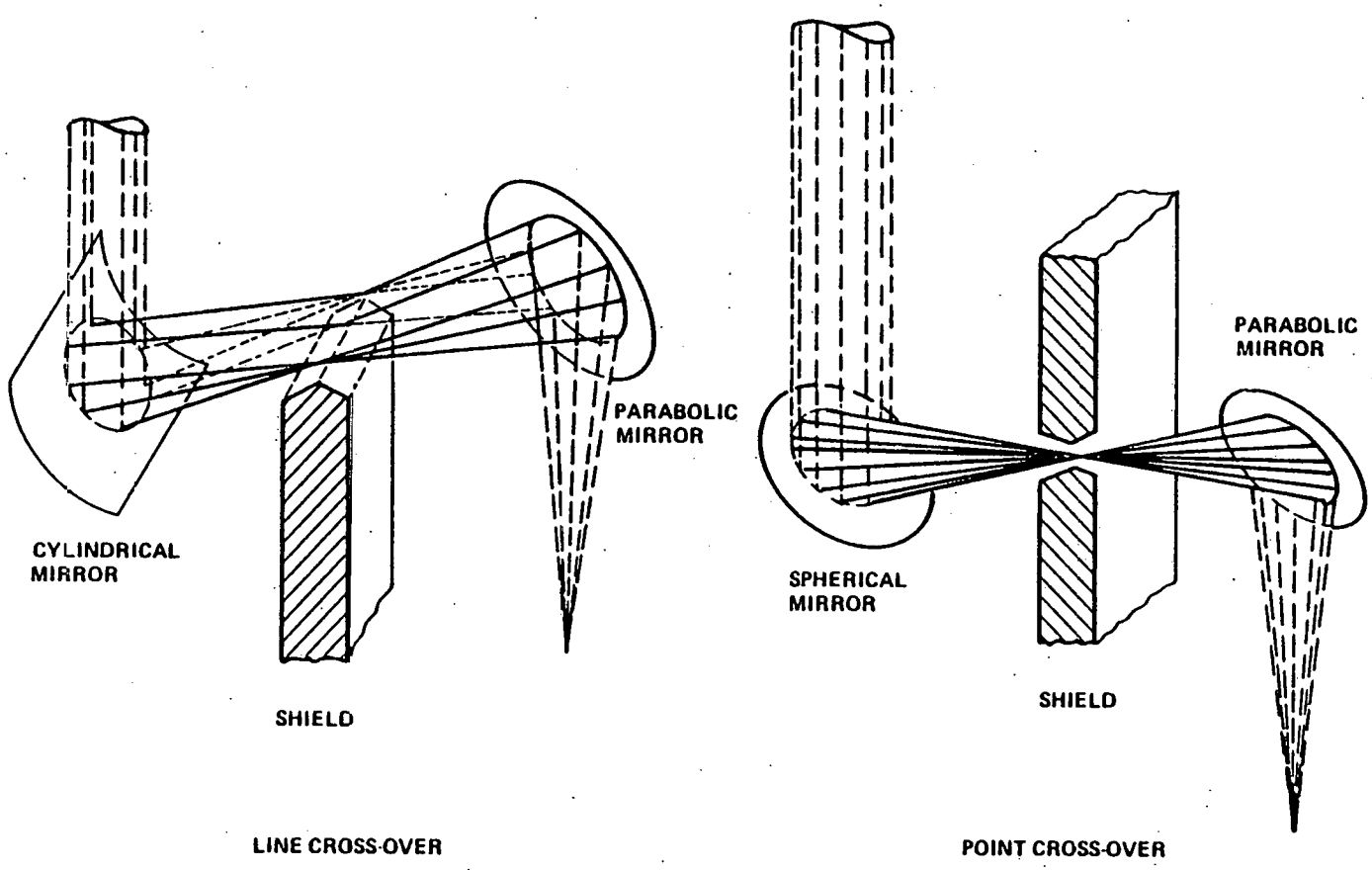

Figure 8. Beam Cross Over Systems.

LITERATURE CITED

1. L. Green, A. Y. Lee, and J. Jedruch, "Neutronic and Thermal Performance of a Blanket Design for an Inertial Confinement Fusion Commercial Power Reactor," Task No. DE-AC08-79DP40086, unpublished.

2. M. M. H. Ragheb, A. C. Klein, and C. W. Maynard, "Three Dimensional Neutronics Analysis of the Mirror-Beam Duct Shield System for a Laser Driven Power Reactor," UWFDM-239, Fusion Research Program, Nuclear Engineering Dept., University of Wisconsin.

3. J. E. Howard, "Imaging Properties of Off-Axis Parabolic Mirrors," UWFDM-214, Nuclear Engineering Dept., University of Wisconsin.

4. Los Alamos Monte Carlo Group, "MCNP - A General Monte Carlo Code for Neutron and Photon Transport, Version 2A," November 1979.

5. Inertial Confinement Fusion Central Station Electric Power Generating Plant, Final Report for the Period March 1, 1979 - Sept. 30, 1980, DOE/DP/40086-1, Vol. I.

APPENDIX A

PART ONE

DATA ON SOLASE BLANKET AND LD/NA SYSTEM

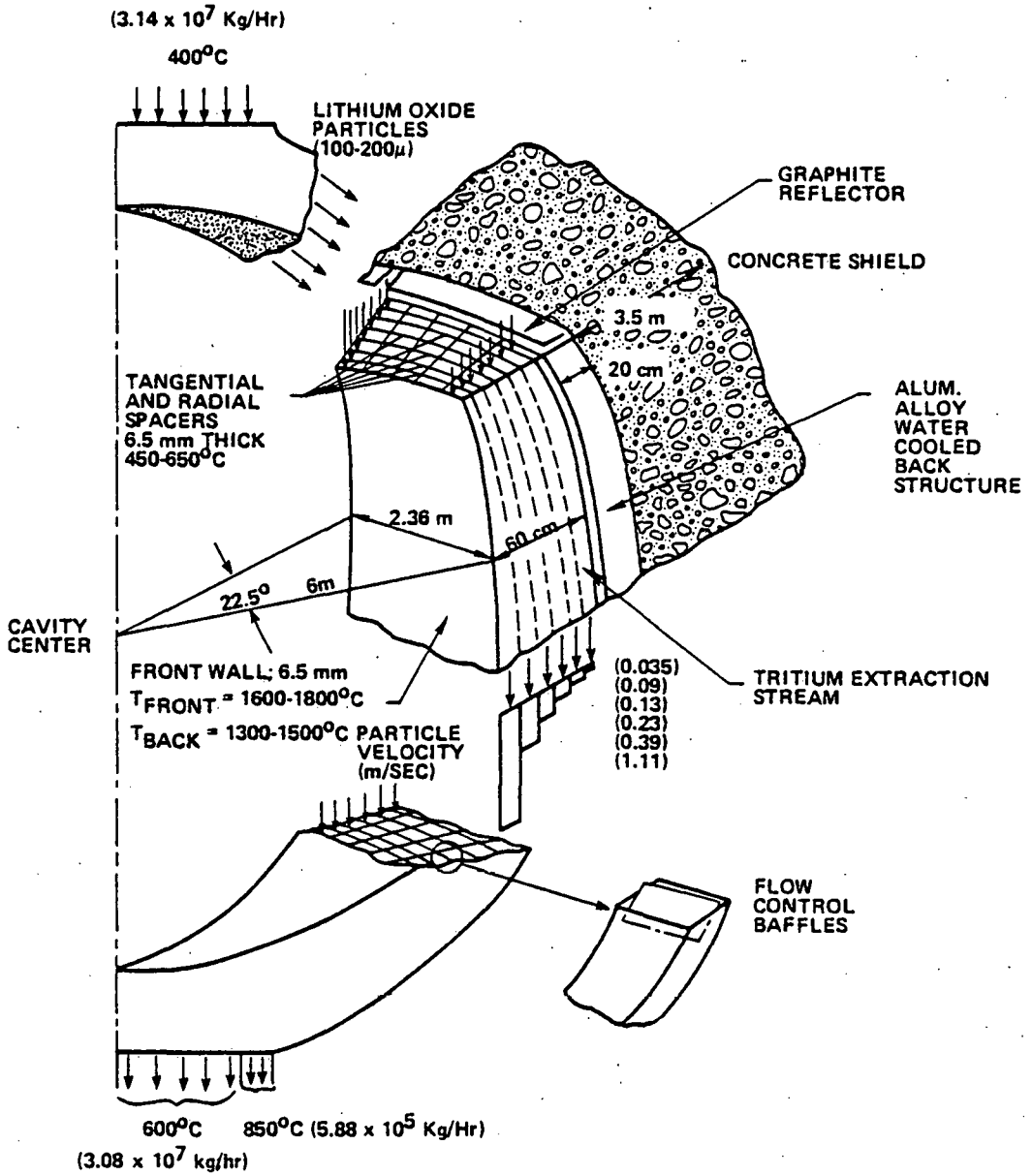

Figure A-1. Schematic Diagram of a SOLASE Blanket Segment.

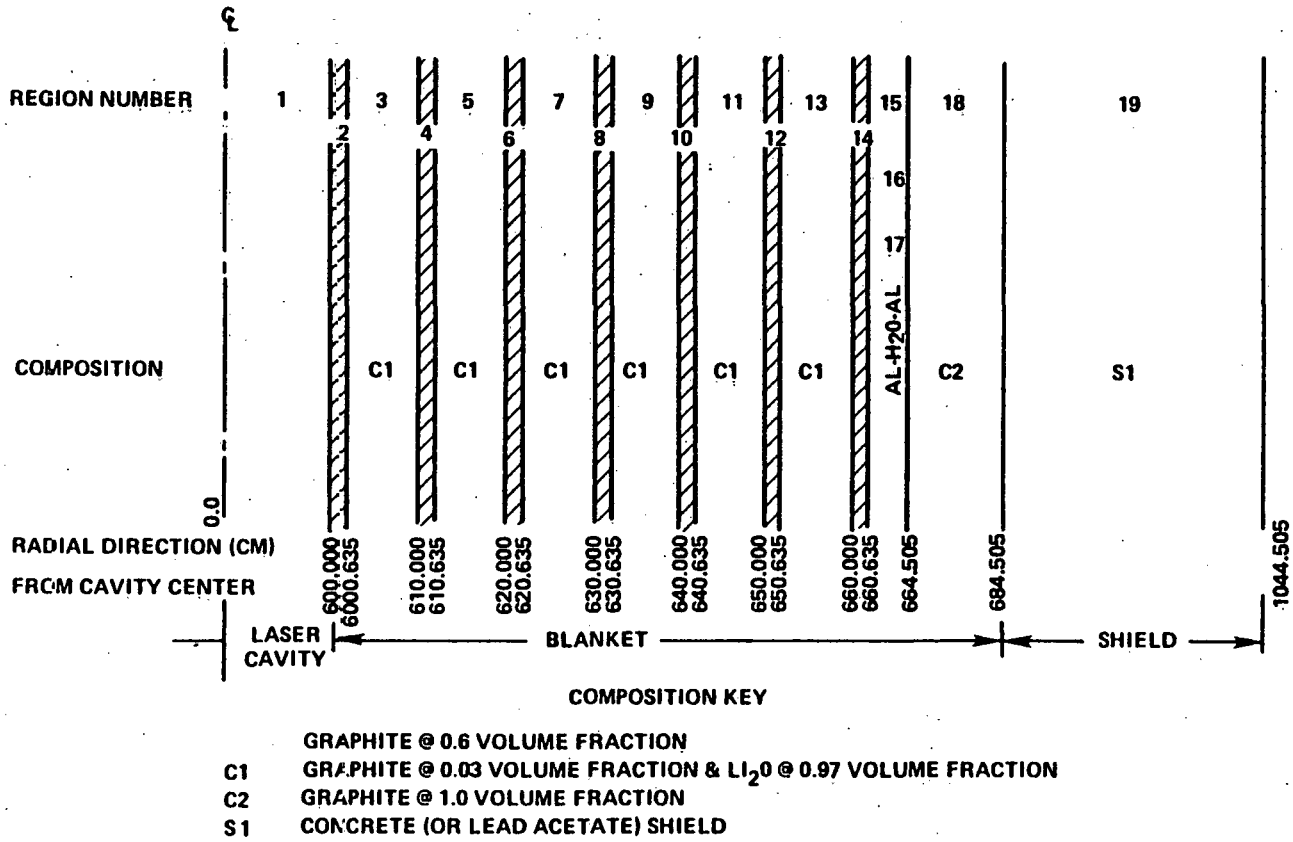

Figure A-2. One-Dimensional Schematic of SOLASE Blanket.

TABLE A-I

Complex SOLASE Blanket Model for Neutronics Analysis

Zone. No.	Thickness (mm)	Material Composition	Density Factor
1	6000	Vacuum	0.0
2	6.35	Graphite	0.6
3	93.65	3% Graphite + 97% Li_2O	0.6
4	6.35	Graphite	0.6
5	93.65	3% Graphite + 97% Li_2O	0.6
6	6.35	Graphite	0.6
7	93.65	3% Graphite + 97% Li_2O	0.6
8	6.35	Graphite	0.6
9	93.65	3% Graphite + 97% Li_2O	0.6
10	6.35	Graphite	0.6
11	93.65	3% Graphite + 97% Li_2O	0.6
12	6.35	Graphite	0.6
13	93.65	3% Graphite + 97% Li_2O	0.6
14	6.35	Graphite	0.6
15	12.70	Al	1.0
16	25.0	H_2O	0.5
17	1.0	Al	1.0
18	200	Graphite	1.0
19	1000	Concrete	1.0
20	2960	Concrete	1.0

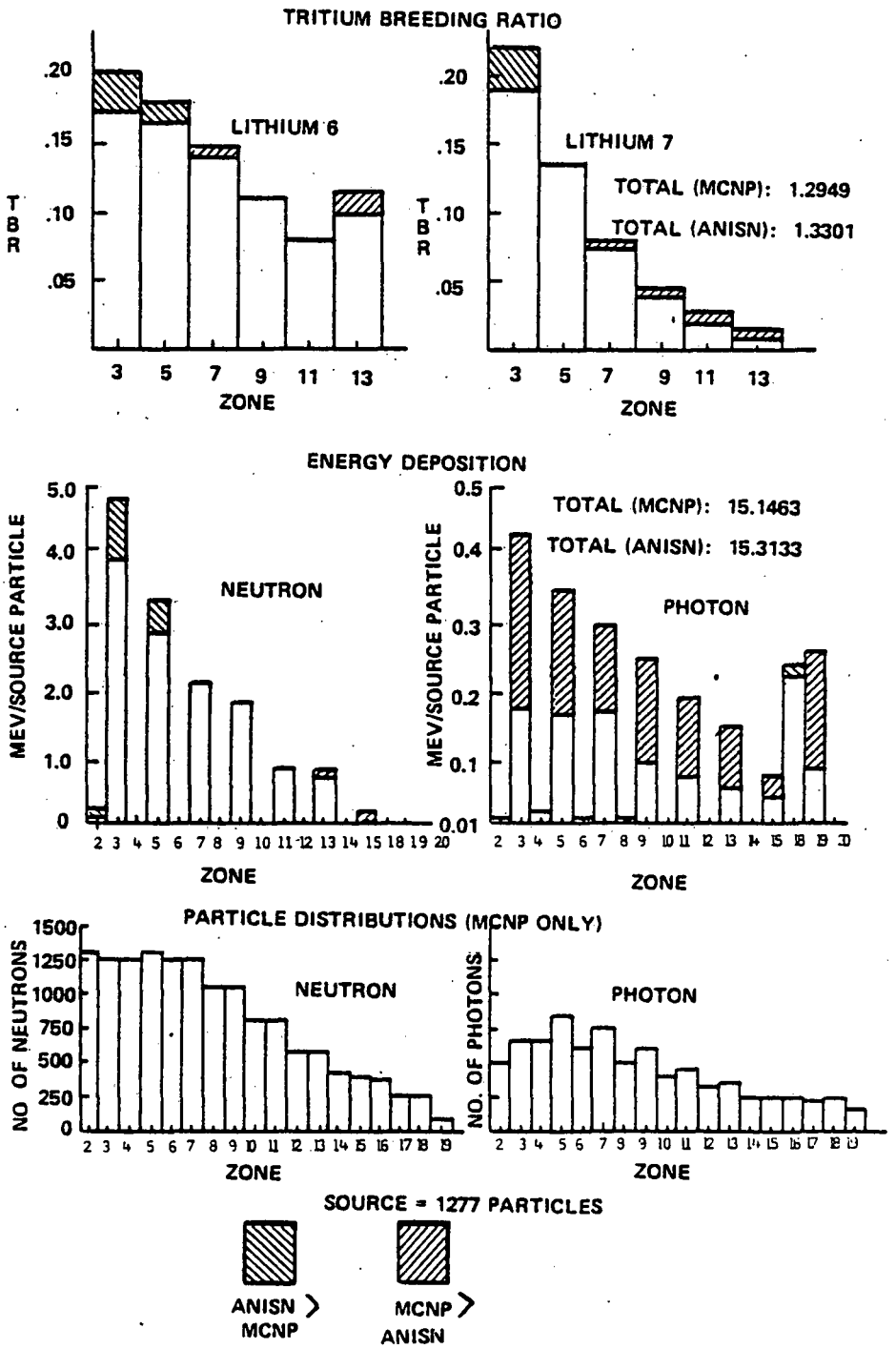

Figure A-3. SOLASE Blanket Results.

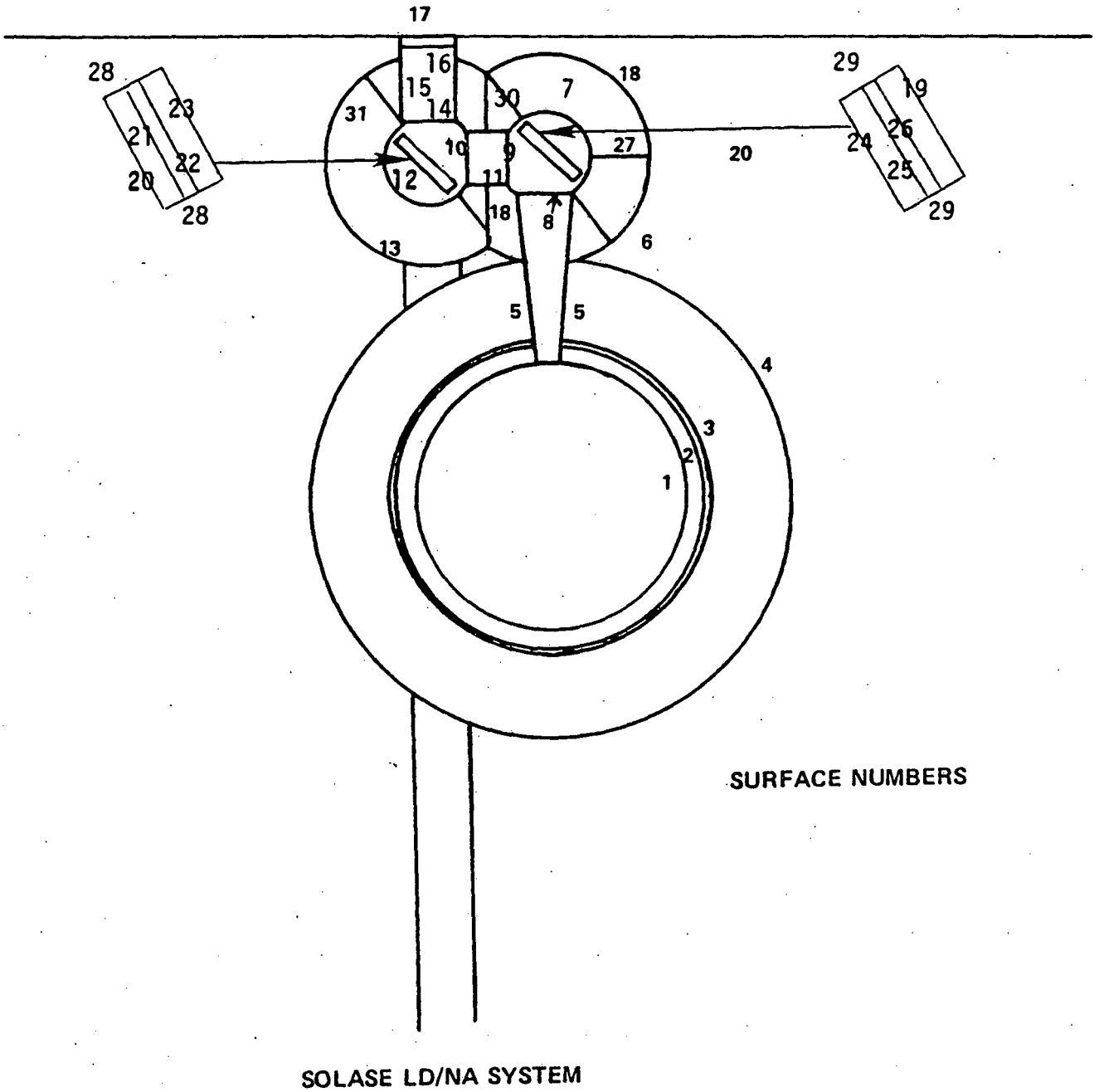

Figure A-4. SOLASE Laser Duct/Neutron Attenuation System.

TABLE A-II

SOLASE LD/NA SYSTEM

(3000 MW Reactor)

Surface	Neutron Fluxes ($n/cm^2/sec$)	Relative Standard Deviation
8	5.030 E 13	.3%
9	3.405 E 12	3.9%
10	1.492 E 12	5.6%
14	3.256 E 11	9.3%
16	8.833 E 10	13.1%
17	2.451 E 9	21.7%
5	9.100 E 11	5.3%
6	1.162 E 9	30.5%
7	7.822 E 12	1.0%
11	1.697 E 12	5.3%
12	3.801 E 11	6.2%
13	1.188 E 8	35.0%
15	1.118 E 11	9.8%
18	3.664 E 10	17.7%
19	1.545 E 13	1.1%
20	3.941 E 11	7.4%
21	4.743 E 11	7.2%
22	5.559 E 11	6.9%
23	6.795 E 11	6.6%
24	2.751 E 13	.5%
25	2.426 E 13	.7%
26	1.863 E 13	1.0%
27	1.052 E 11	8.6%
28	9.998 E 12	1.9%
29	3.833 E 11	7.8%

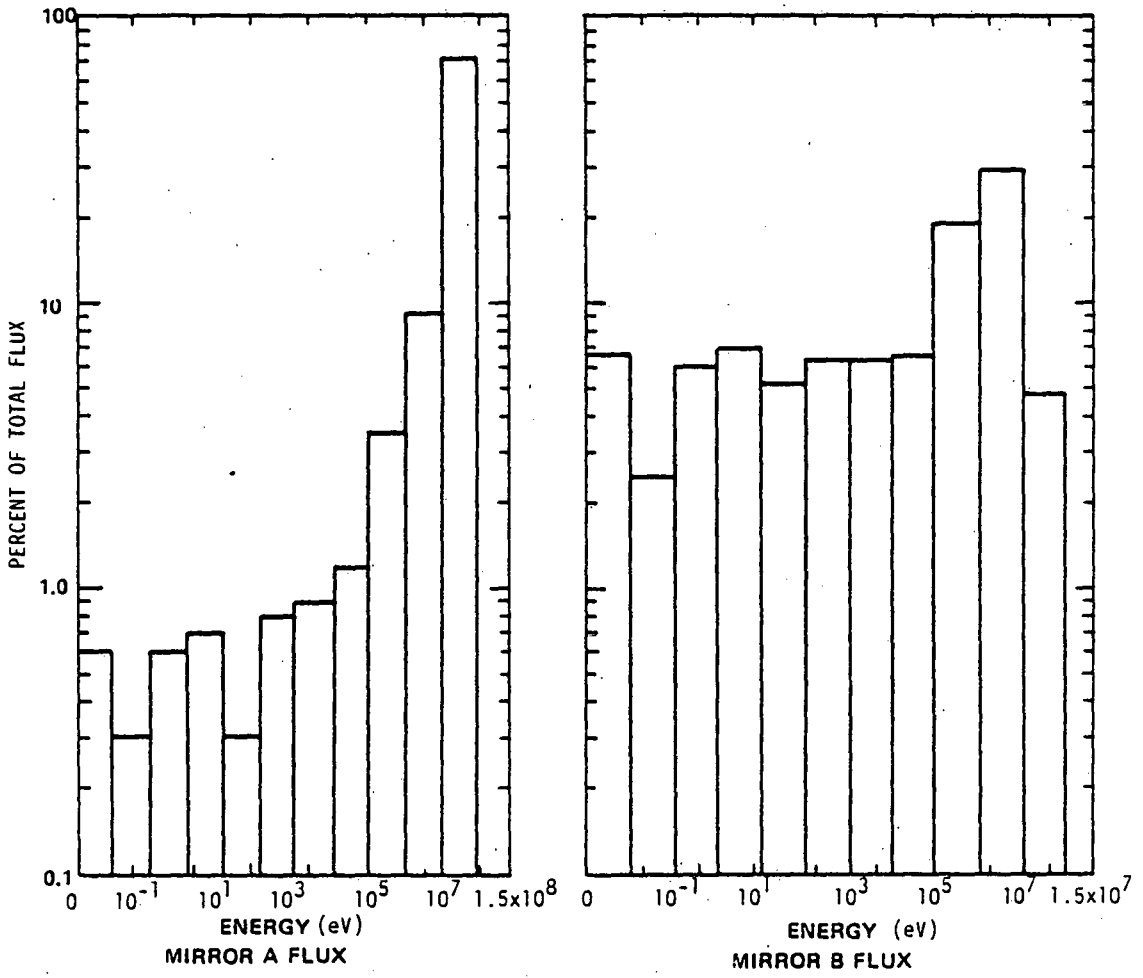

Figure A-5. Percent of Total Flux vs. Energy, SOLASE System.

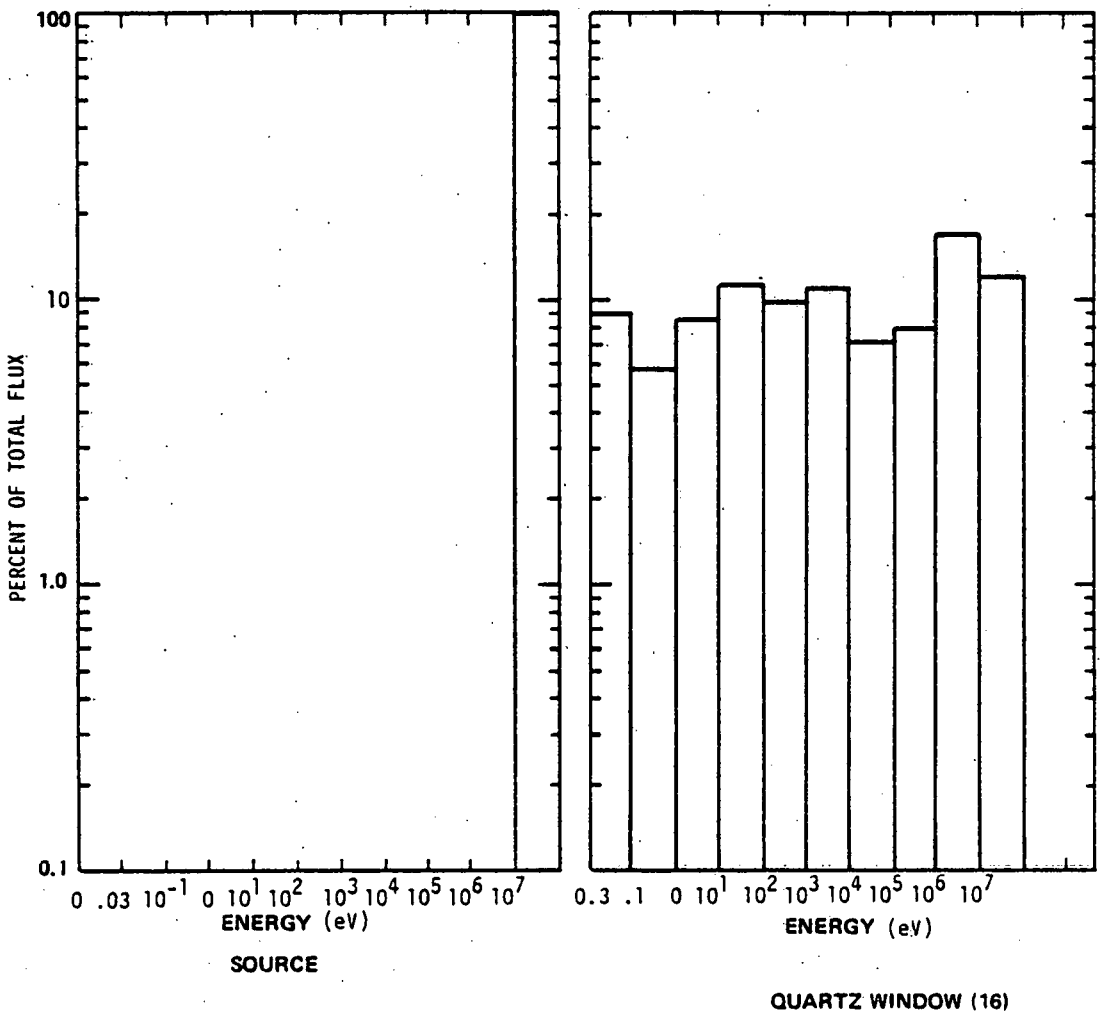

Figure A-6. Percent of Total Flux vs. Energy, SOLASE System.

PART TWO

DATA ON WESTINGHOUSE BLANKET AND LD/NA SYSTEM

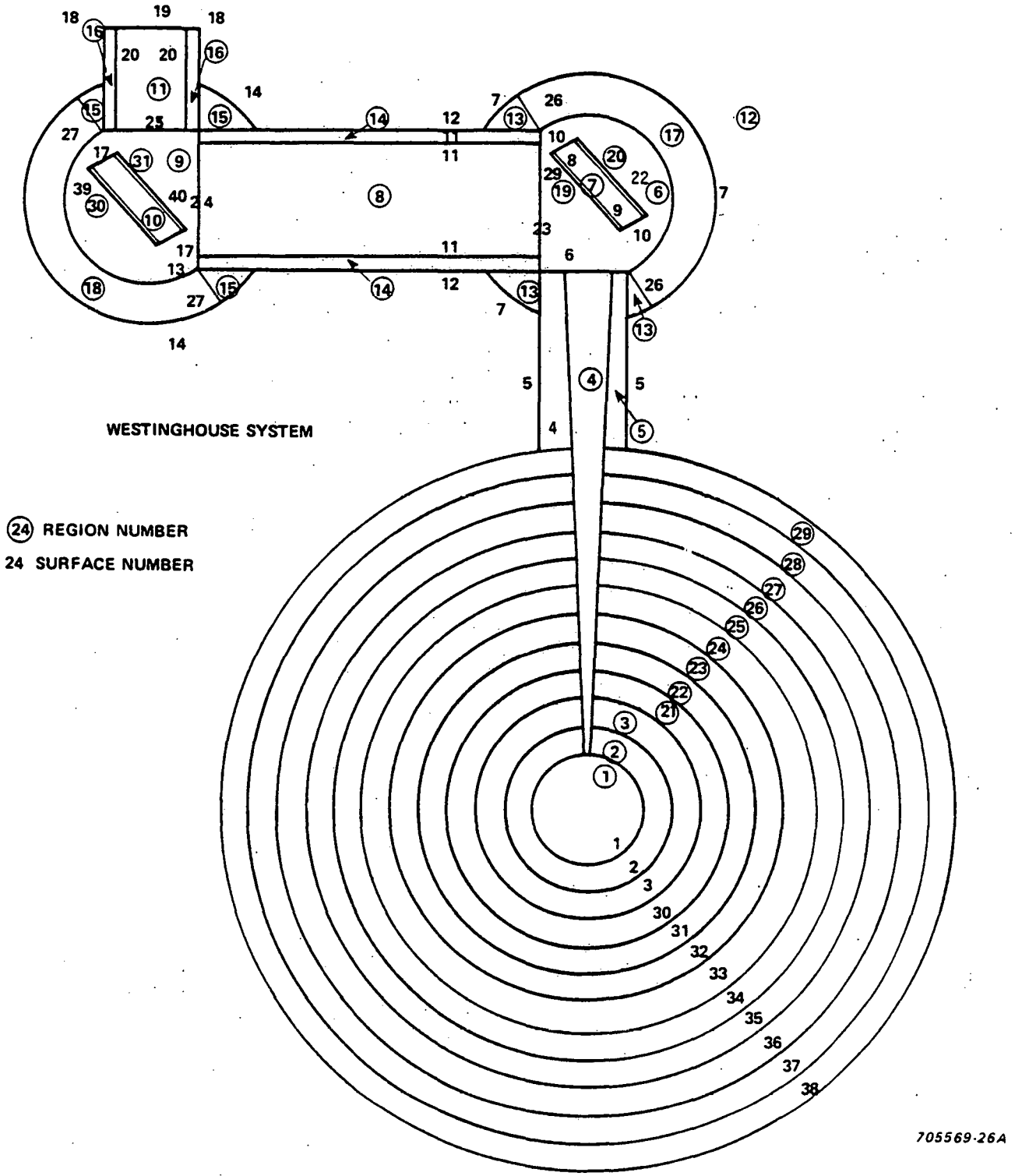

Figure A-7. Westinghouse Blanket and Beam Duct System.

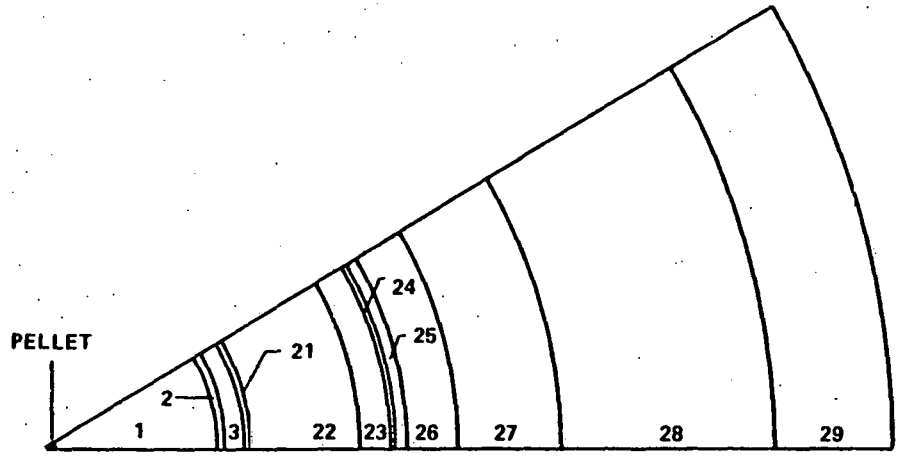

ZONE	COMPOSITION	THICKNESS (METERS)
1	CHAMBER (VOID)	10.0
2	Ta COATING	0.01
3	Li IN HT-9 TUBES	0.12
21	HT-9 STEEL SUPPORT	0.02
22	Li + 4 v/o STRUCTURE	0.58
23	GRAPHITE REFLECTOR + 10 v/o STRUCTURE	0.20
24	Li + 4 v/o STRUCTURE	0.02
25	STEEL SHELL	0.025
26	THERMAL INSULATION	0.305
27	CONCRETE + 5 v/o IRON	1.0
28	MACHINERY SPACE (VOID)	7.7
29	CONCRETE + 5 v/o IRON	2.0

Figure A-8. Westinghouse Blanket Model.

TABLE A-III

MATERIALS IN WESTINGHOUSE
BLANKET AND LD/NA DESIGN

Material	How it was Simulated for MCNP
Tantalum	100% Tantalum
Li in HT-9 tubes	lithium (p = .5 g/cc) + 3 v/o iron (p = 7.8 g/cc) weight percents: iron, 32.8%, Li7, 62.8%, Li6, 4.4%
HT-9 Steel	100% Iron
Li + 4 v/o Structure	Lithium + 4 v/o iron w/o: 29.7% iron, 56.4% Li7, 3.9% Li6
Steel Shell	100% Iron
Thermal Insulation	a/o: 63.8% 016, 19.9% Si, 17.2% Al 27
Concrete w/ 5 v/o Iron	a/o: iron 3.5%, calcium 24.33%, silicon 8.24%, 016 32.96%, carbon 12 4.7%, hydrogen 43.67%
Concrete Shielding (not in blanket)	w/o: calcium 24.33%, oxygen 46.7%, silicon 20.24%, carbon 4.92%, hydrogen 83%, boron (natural isotopic ratios) 3%
Aluminum	100% aluminum
Pellet	a/o: 50% D, 50% T

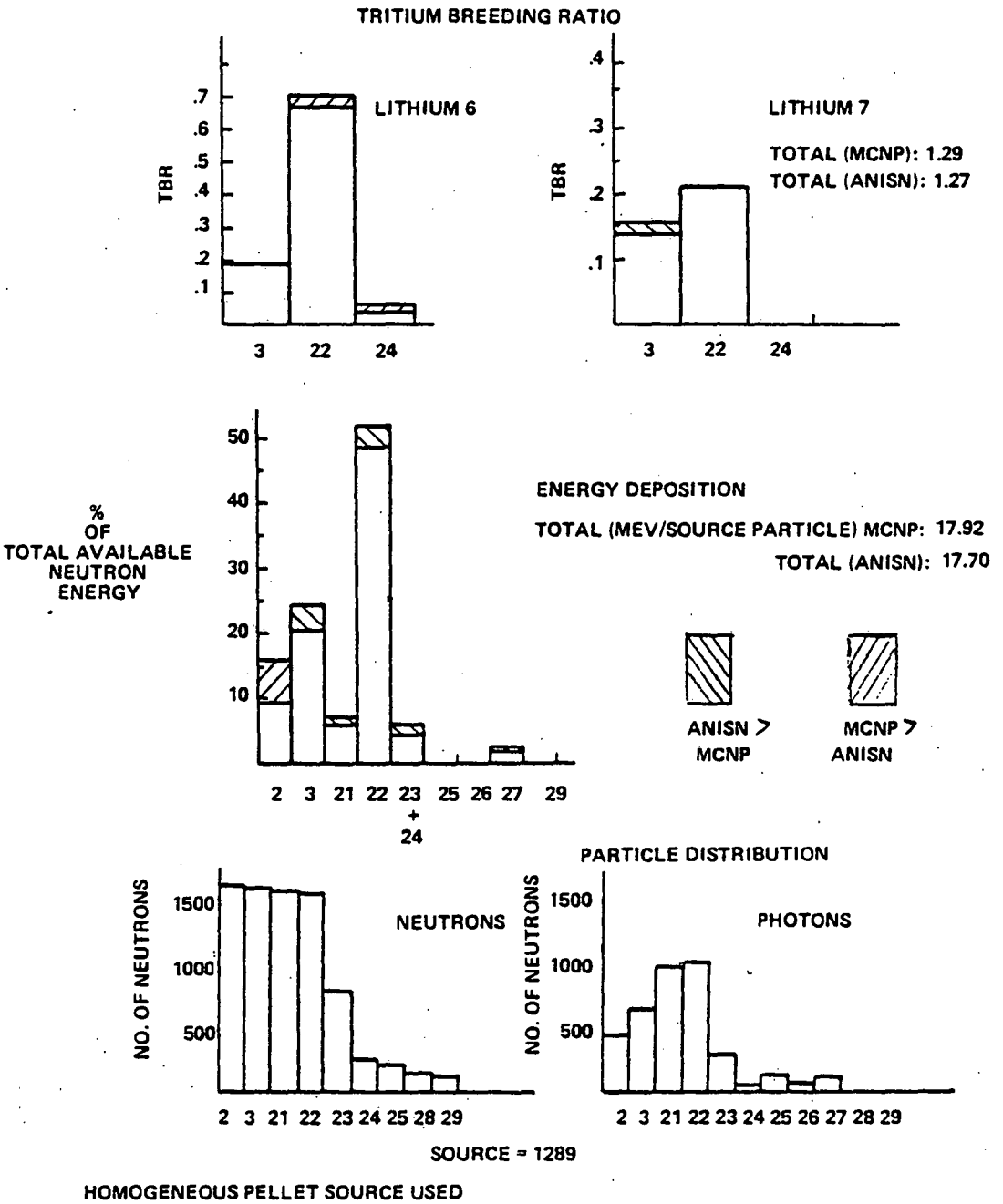

Figure A-9. Comparison of MCNP and ANISN Results for Westinghouse Blanket Design.

TABLE A-IV

TIME (sec)	2E-7	2.2E-7	2.4E-7	2.8E-7	4E-7	1E-6	5E-6	1E-5	1E-5	5E-5	1E-4	.001	.005	.01	.1	
2	5.105 E-10 14.1	3.546 E-10 2.7	2.258 E-10 21.4	1.202 E-10 19.8	7.843 E-11 25.9	7.541 E-11 33.4	2.507 E-12 100	1.543 E-10 60.1	0 0	0 0	2.727 E-12 100	0 0	0 0	0 0	0 0	0 0
3	7.266 E-10 12.5	5.168 E-10 17.7	1.948 E-10 21.1	1.47 E-10 18.4	1.172 E-10 17.9	1.147 E-10 20.2	9.644 E-11 23.3	2.038 E-12 100	5.36 E-11 47.5	0 0	0 0	3.751 E-12 100	0 0	0 0	0 0	0 0
21	1.19 E-9 11.7	6.265 E-10 12.8	2.835 E-10 16.5	1.897 E-10 19.5	2.000 E-10 19.6	1.122 E-10 17.0	2.251 E-11 26.0	9.055 E-12 71.5	4.531 E-11 56.1	3.092 E-13 100	4.576 E-14 100	5.051 E-12 100	1.441 E-12 100	0 0	0 0	0 0
22	2.268 E-10 14.2	5.183 E-10 9.9	1.188 E-10 13.5	1.048 E-10 18.4	5.625 E-11 19.0	6.54 E-11 19.9	4.476 E-11 30.3	9.244 E-12 77.7	2.801 E-11 56.2	1.875 E-12 55.4	7.997 E-12 60.9	3.508 E-12 100	6.033 E-12 100	0 0	0 0	0 0
23	2.109 E-11 50.1	1.681 E-10 19.3	5.397 E-11 32.2	2.344 E-11 40.8	4.863 E-12 38.9	1.292 E-11 60.4	5.95 E-11 41.9	8.517 E-12 54.2	6.728 E-11 33.5	2.748 E-11 47.7	5.696 E-11 38.5	7.246 E-12 67.0	1.032 E-11 79.0	0 0	0 0	0 0
24	1.153 E-11 76.2	5.858 E-11 35.4	1.167 E-11 63.4	6.409 E-12 100	0 0	6.242 E-12 80.4	221 E-11 76.6	1.977 E-11 59.4	6.212 E-11 41.7	3.792 E-11 44.6	4.07 E-11 40.7	1.477 E-11 82.9	1.638 E-11 71.6	0 0	0 0	0 0
25	1.087 E-11 99.8	5.021 E-11 41.3	1.134 E-11 57.7	1.47 E-11 62.6	4.988 E-12 88.2	6.131 E-12 94.5	4.72 E-11 56.7	2.599 E-11 53.0	5.991 E-11 45.4	7.29 E-11 35.3	8.085 E-11 35.5	2.641 E-11 55.3	1.902 E-11 67.0	0 0	0 0	0 0
26	3.655 E-12 100	3.369 E-11 38.5	2.843 E-11 50.3	1.57 E-11 59.4	2.89 E-12 100	5.156 E-12 100	4.086 E-11 98.5	1.312 E-11 65.5	4.23 E-11 45.3	8.561 E-11 40.9	1.334 E-10 41.3	9.22 E-11 77.8	3.801 E-12 89.1	0 0	0 0	0 0
27	0 0	3.354 E-12 52.5	3.552 E-12 69.2	2.771 E-13 86.7	2.79 E-13 86.9	8.951 E-13 100	2.369 E-13 100	2.157 E-12 85.4	1.851 E-11 38.8	9.152 E-12 49.2	1.266 E-11 27.4	5.836 E-12 37.8	1.717 E-12 76.2	0 0	0 0	0 0
29	0 0	0 0	0 0	0 0	0 0	0 0	0 0	0 0	0 0	0 0	0 0	0 0	0 0	0 0	0 0	0 0

PHOTON ENERGY DEPOSITION WITH TIME (MeV/Gram/Source Particle, Relative Standard Deviation, %)
WESTINGHOUSE BLANKET [Pellet Source]

TABLE A-V

REGION	TIME (sec) 2E-7	2.2E-7	2.4E-7	2.8E-7	4E-7	1E-6	5E-6	1E-5	5E-5	1E-4	5E-4	1E-3	5E-3	.01	.100	
	2	1.575 E-9 3.7	4.532 E-10 8.4	2.326 E.10 12.5	3.083 E-10 10.5	3.976 E-10 9.8	7.565 E-10 8.1	1.699 E-9 5.0	9.426 E-10 7.1	2.021 E-9 7.9	2.494 E-10 26.7	9.264 E-11 32.7	8.228 E-11 93.0	3.155 E-11 50.2	3.080 E-11 100	0 0	0 0
	3	7.991 E-9 3.2	3.23 E-9 6.2	1.404 E-9 7.7	1.215 E-9 8.5	1.526 E-9 8.2	2.242 E-9 6.8	4.328 E-9 4.1	1.417 E-9 7.2	1.471 E-9 8.4	1.402 E-10 41.9	2.057 E-10 37.4	1.833 E-11 100	7.822 E-11 59.6	8.620 E-12 100	0 0	0 0
	21	7.869 E-10 4.5	1.729 E-10 8.1	5.84 E-11 10.2	3.076 E-11 14.3	2.331 E-11 10.7	4.074 E-11 13.0	3.382 E-11 6.3	3.413 E-12 10.6	1.184 E-12 12.0	5.085 E-14 89.9	5.374 E-15 58.3	0 0	0 0	0 0	0 0	0 0
	22	8.956 E-10 5.2	2.105 E-9 5.1	7.057 E-10 7.1	6.135 E-10 5.2	7.347 E-10 4.3	1.045 E-9 3.8	2.308 E-9 7.1	7.487 E-10 8.5	6.771 E-10 36.5	4.751 E-11 40.0	3.332 E-11 0	0 0	0 0	0 0	0 0	0 0
	23	0 0	1.079 E-10 18	6.428 E-11 17.4	4.087 E-11 14.9	3.17 E-11 15.2	2.544 E-11 22.3	1.477 E-11 12.6	1.134 E-12 18.7	8.465 E-13 17.4	3.792 E-13 14.3	8.053 E-13 21.4	9.135 E-14 69.2	2.463 E-14 100	0 0	0 0	0 0
	24	0 0	3.966 E-11 45.6	3.516 E-11 46.0	3.989 E-11 32.3	4.164 E-11 38.9	1.913 E-10 20.9	1.443 E-9 16.3	1.968 E-9 19.3	4.257 E-9 17.2	7.499 E-10 35.1	7.043 E-10 39.3	0 0	0 0	0 0	0 0	0 0
	25	0 0	4.771 E-12 54.4	9.796 E-13 78.3	9.454 E-13 30.9	3.195 E-13 39.5	6.765 E-13 44.6	1.519 E-13 20.2	1.025 E-13 22.2	2.461 E-13 19.1	1.134 E-13 43.2	8.53 E-13 35.0	1.285 E-13 55.1	3.473 E-13 53.8	1.148 E-15 100	0 0	0 0
	26	0 0	1.731 E-11 56.9	7.976 E-12 59.3	8.288 E-12 35.1	8.428 E-12 38.7	6.154 E-12 45.7	2.265 E-13 31.6	5.941 E-14 41.5	6.889 E-14 22.9	1.067 E-13 34.8	7.496 E-13 48.1	1.183 E-12 42.0	8.343 E-12 52.5	5.294 E-12 79.3	2.732 E-12 100	0 0
	27	0 0	7.81 E-13 72.7	4.919 E-12 62.9	1.651 E-12 47.7	1.858 E-12 40.6	4.883 E-13 45.9	4.754 E-14 42.1	1.216 E-14 22.3	1.691 E-13 15.8	3.893 E-13 14.0	1.775 E-12 15.8	4.386 E-13 29.7	1.102 E-13 66.9	0 0	0 0	0 0
	29	0 0	0 0	0 0	0 0	0 0	0 0	0 0	0 0	0 0	0 0	0 0	0 0	0 0	0 0	0 0	0 0

NEUTRON ENERGY DEPOSITION WITH TIME (MeV/Gram/Source Particle, Relative Standard Deviation, %)
WESTINGHOUSE BLANKET [Pellet Source]

TABLE A-VI

WESTINGHOUSE BLANKET

Zone	Mass (g)
2	2.088 E8
3	1.070 E8
21	2.015 E8
22	6.277 E8
23	6.588 E8
24	2.376 E7
25	2.945 E8
26	4.746 E7
27	4.536 E9
29	2.878 E10

TABLE A-VII

WESTINGHOUSE LD/NA SYSTEM

3500 MW

Surface	Neutron Flux ($n/cm^2/sec$)	Relative Standard Deviation
4	1.678×10^{12}	4.1%
5	2.913×10^{11}	5.8%
6	4.244×10^{13}	4.7%
7	3.315×10^{11}	4.4%
8	5.923×10^{14}	.3%
9	4.411×10^{14}	.5%
10	1.917×10^{14}	1.0%
11	9.746×10^{11}	3.6%
12	2.304×10^{11}	3.6%
13	9.437×10^{9}	78.5%
14	0	-----
15	2.508×10^{10}	87.4%
16	2.733×10^{10}	85.7%
17	7.685×10^{9}	74.2%
18	2.504×10^{7}	70.7%
19	1.505×10^{6}	100%
20	2.782×10^{8}	73.1%
21	0	-----
22	4.848×10^{14}	0.2%
24	3.869×10^{10}	78.2%
25	6.761×10^{9}	71.9%
39	2.273×10^{10}	87.4%
40	3.000×10^{10}	85.6%
41	4.427×10^{13}	1.3%
42	6.402×10^{14}	.5%
43	4.560×10^{10}	70.7%
28	4.001×10^{14}	.5%
29	6.424×10^{14}	.2%
23	3.362×10^{13}	3.1%

TABLE A-VIII

WESTINGHOUSE LD/NA SYSTEM

14 MEV MONOENERGETIC SOURCE, CONE SOURCE

Cell	MeV/Source Particle			
	n		γ	
2	1.847	3.0%	.378	10.1%
3	2.705	1.7%	.212	7.9%
5	1.455E-5	5.9%	1.293E-5	5.3%
7	2.242E-5	1.2%	3.376E-6	5.3%
10	<1.05E-6	0	1.648E-9	96.4%
13	7.497E-6	5.6%	6.928E-6	5.6%
14	7.150E-6	5.8%	6.041E-6	5.9%
15	<1.05E-6	0	5.650E-11	100%
16	<1.05E-7	0	2.193E-10	100%
17	4.538E-5	2.4%	3.183E-5	2.6%
18	<1.05E-6	0	1.985E-8	95.0%
19	2.98E-5	.7%	5.38E-6	14.6%
20	1.881E-5	1.9%	3.86E-6	13.2%
21	.233	3.1%	.557	6.6%
22	6.184	2.1%	.757	6.3%
23	.191	10.2%	.346	11.5%
24	.223	11.2%	.00721	16.2%
25	.00286	28.6%	.127	15.5%
26	.00316	27.3%	.0238	22.3%
27	.0572	29.7%	.265	17.8%
29	<7.63E-4	0	<5.45E-4	0
30	<1.05E-6	0	1.641E-9	96.2%
31	<1.05E-6	0	1.974E-9	96.5%
33	4.201E-4	.9%	1.208E-4	1.6%

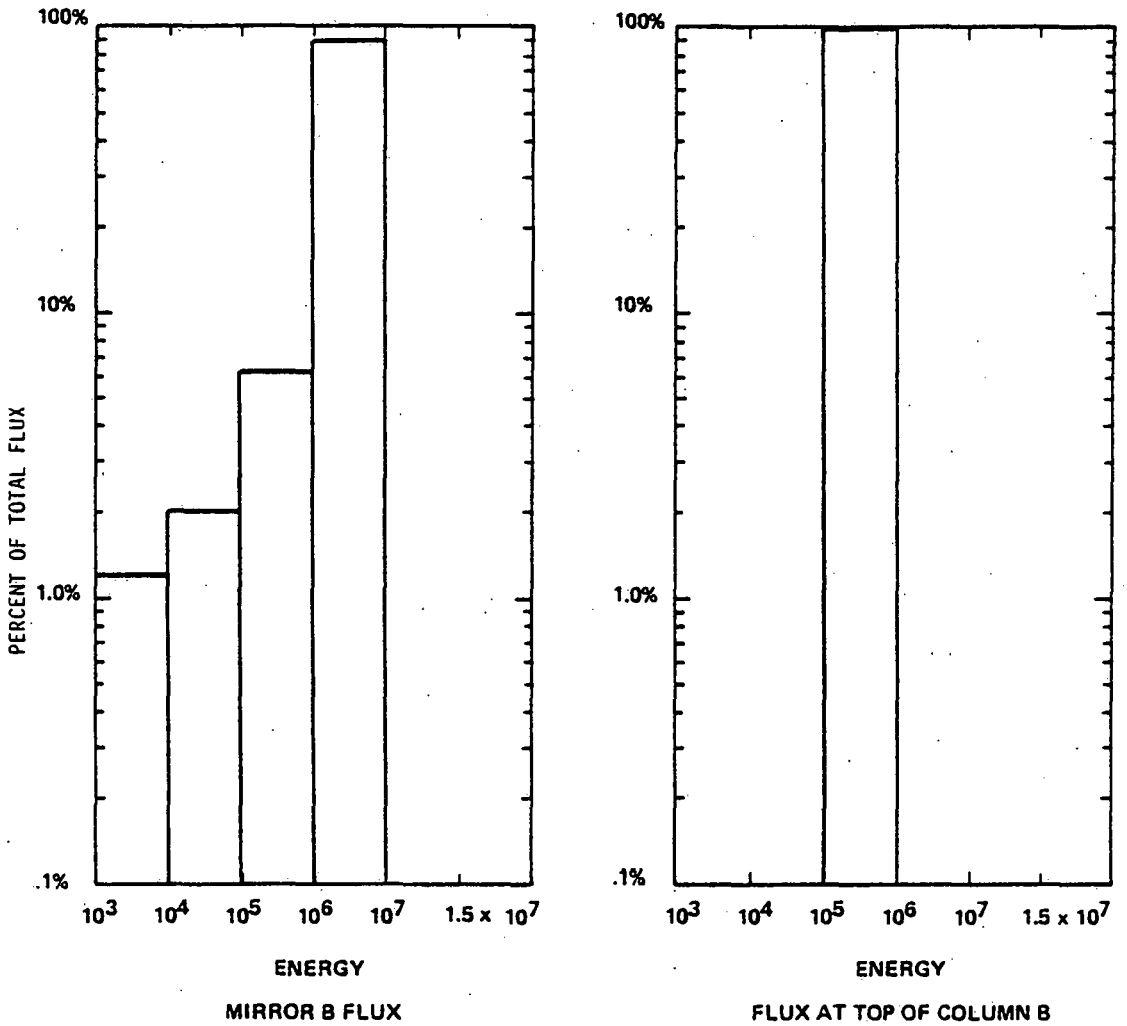

Figure A-10. Percent of Total Flux vs. Energy, Westinghouse Laser Duct/ Neutron Attenuation System.

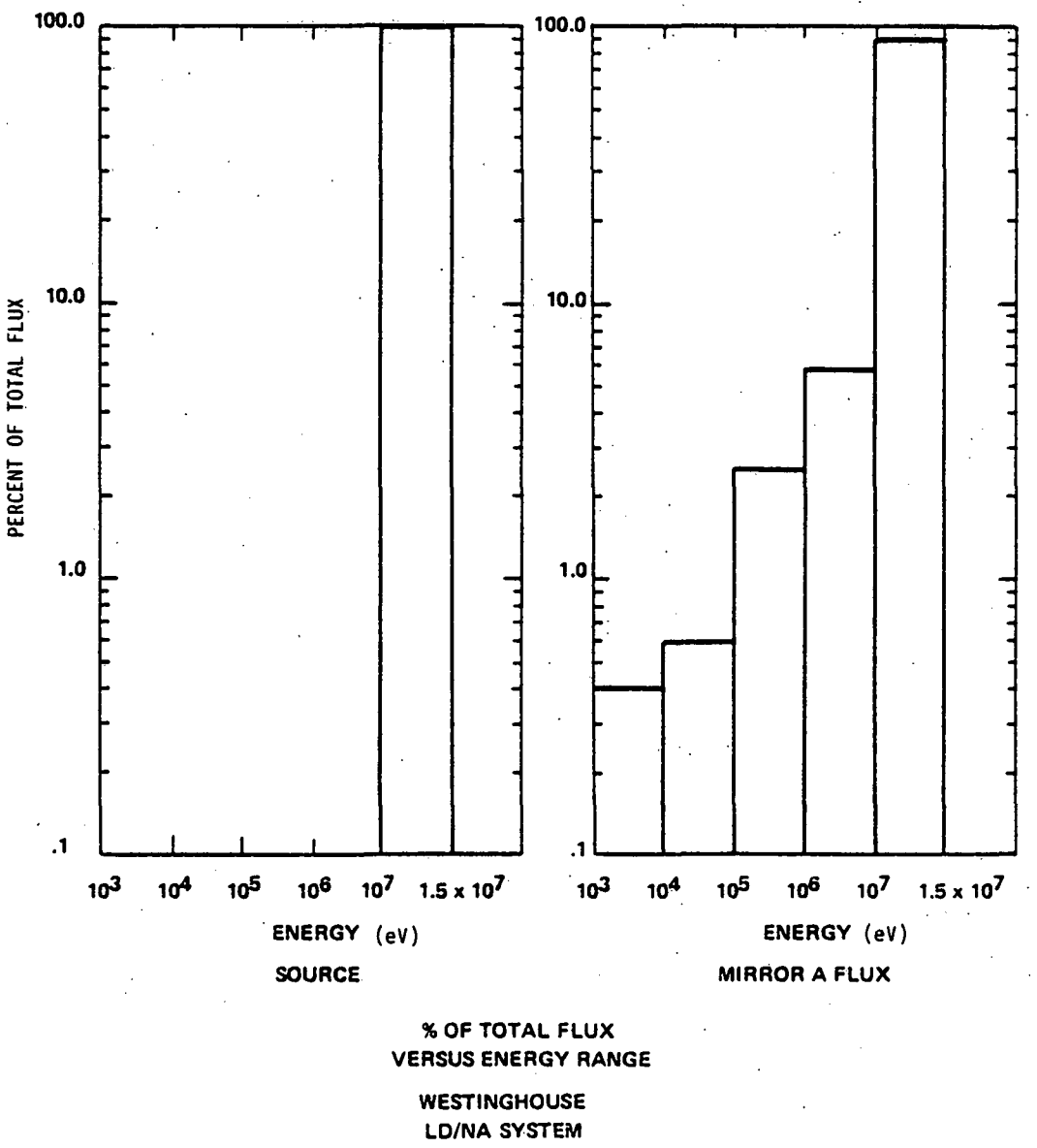

Figure A-11. Percent of Total Flux vs. Energy, Westinghouse Laser Duct/ Neutron Attenuation System.

APPENDIX B

APPENDIX B

Shortcomings of MCNP

MCNP is a well documented code that is easy to use. It has only a few shortcomings, such as:

1) It does not Doppler broaden any cross sections. This is important for high Z problems with high temperatures. To use Doppler broadened cross sections, personnel at Los Alamos Laboratory can alter the cross section file on an individual basis, but this takes time.
2) Lattice work is impractical, as every rod and clad would have to be numbered.
3) Certain shapes are difficult to represent without adding several additional surfaces (specifically, bounding the end of a cylindrical volume with a spherical surface).
4) Interaction rates (such as the tritium breeding ratio) are cumbersome to calculate.
5) The manual does not have a chapter specifically on errors.

If one does not know how to use MCNP, or are knowledgeable of other Monte Carlo codes that have computational capability of the type that MCNP is weak in (some of the weaknesses are listed above), consider using another code.

The next section is written as a supplement to the manual, not a replacement for it. It will be useless unless one is familiar with the format and structure of MCNP input decks.

Error Messages

Fatal Errors & Warnings

Fatal errors are by far the easiest to correct. There are basically two types: geometric and nongeometric. Geometric fatal errors are caused by errors in the cell cards, and usually occur the first time an input deck is run which has other side cells listed (see p. 119 of manual). They can be corrected by examining each card associated with the cells listed in the error message. Other fatal geometric errors include wrong signs on surfaces, missing commas, spaces or digits, failure to list all the surfaces, missing surface cards, etc.

Nongeometric fatal errors are difficult to discuss in general but are specified in the error message. Some common nongeometric fatal errors are: 1) number of entries on importance cards do not match number of cells; 2) failure to open cross section files; 3) tally cards with the same number.

Warnings are not the same thing as errors. They indicate a condition which could be the result of a mistake in the input file, but could be a necessary part of the problem. The more common warnings occur when:

1) The energy bounds of the cross section files are not specified by the user. The default value is zero, which is below the bottom of the cross section tables.
2) Gamma production cross sections are missing for some isotopes in the problem.
3) The atomic fractions on the material cards don't add to one and have to be normalized.
4) The volumes or areas of some cells cannot be computed by MCNP and the user did not specify them. MCNP then assumes a volume or area of one.

Lost Particles (Geometry error in NEWCEL)

Lost particles are the second most common error. Lost particles always indicate that the geometry was incorrectly specified. When this error occurs, check the plot of the geometry. The great majority of the time, the plot will show where the geometry was ill-specified. If it does not, then the problem ill-specificity is too small to appear on the plot. Often this occurs at corners, where different surfaces meet. Blow them up using the ZOOM feature of the plot program and check them.

MCNP will automatically terminate the run when ten particles get lost. If less than ten are lost, MCNP will print out a history of the lost particles and continue the run. See Chapter 4 for interpretation of lost particle histories. The point at which the particles are lost (listed in the particle history) tells you where the geometry is ill-specified. If ten particles get lost, the geometry error is probably big enough to correct. If less than ten are lost, the error is probably small enough to ignore.

Error in TIMINT

This error occurs when the history of a single particle is greater than twenty seconds. If a particle has been increased in importance 10,000 times, for example, (creating 9,999 new particles) the lifetime from creation to extinction for each of the 10,000 particles must sum to less than 20 seconds, or MCNP will automatically terminate. The only solution to this problem is to keep the importance of any one cell $\leq$ 10,000.

These are the only terminating errors I encountered.

Tips in Usage of MCNP

The following tips on using MCNP will save you a lot of frustration. They are for specific calculations or problems that I encountered in the

course of my project.

1) For a neutron only problem (MODE 0, the default) QED can be used to obtain the output file. For a neutron/photon or photon only problem, TRIX AC must be used to obtain the entire output file. All output files are 130 characters wide, and are difficult to read when printed on an 80 character terminal. To get them printed correctly on a 130 ch. terminal, type LW 130 (when prompted by a hyphen in QED) or TTY7,130 (when prompted by a period in TRIX AC) when using the LLL system.

2) To calculate the tritium breeding ratio, and other reaction rates per source particle, use a tally multiplier card (p. 146 of manual). The R number of the specific reaction you are interested in can be found in Appendix F of the manual. The material card associated with the material number must list only the material that the reaction occurs in. This means that the tritium breeding ratio requires 2 tally multiplier cards, one specifying 100% lithium 6 and the other specifying 100% lithium7. To get the reaction rate per source particle (TBR or others), the multiplier in front of the integral (C) must be equal to the total number of atoms of the specific type for the reaction in the cell divided by 10^{24}. The easiest way to get this number is to run MCNP using the IP option (normally used for plotting). The output produced will list atomic fraction, atomic density (for all atoms in a cell regardless of type) and volumes. The total number of atoms divided by 10^{24} can be calculated by multiplying these three values together for a particular isotope in a particular cell. For reaction rate calculations for a particular element, every isotope of the element in every cell must have a tally multiplier card, so for 15 cells containing lithium, 30 tally cards must be used (tally type 4). For details, see the latter part of Appendix B, test case SFTSTL.

3) If you have a cell with a cylindrical wall whose ends are capped

with spheres or cylinders, consider dividing these end spheres or cylinders into hemispheres and using a plane to bound the ends of the cylinders (see Fig. B-1). It is very difficult to get the plot to appear correct otherwise.

4) All energy deposition problems must be run using neutron/photon mode (mode 1). These models cannot be run separately and the results summed. The only cards which must be added to go from neutron to neutron/photon mode is a MODE 1 card after the second blank delimiter and an IP card. For every cell in which energy is deposited, two tally cards must exist, one for neutrons, one for photons. Unless the MCNP code is altered, up to 40 tally cards are allowed. Any more is a fatal nongeometric error.

5) To use more than one tally (even if they are the same type), each tally card must have a different number following F. Neutron tallies of the same type are written in a manner exemplified by this example: if the tally is of type 6, energy deposition, then the first ten tally cards would begin with F6, F26, F46, F66, F86, F106, F126, F146, F166, and F186. For photon tallies of energy deposition, the first 10 tally cards would begin with F16, F36, F56, F76, F96, F116, F136, F156, F176, and F196.

6) If, in your problem geometry, you have a cell completely inside another not contacting any of the bounding surface, and the inside and outside cell are of different shapes or at odd angles with respect to one another, consider learning to use union operators and Godfrey cells (p. 17 of manual). It will be difficult to get the plot to appear correct otherwise.

7) To completely bias a source (producing a cone segment of an isotopic source) you must use the MCNP version available from directory RUNMCNP2A on the CDC 7600. This version is not available on the CRAY 1. If this version of MCNP is used for plotting on the CDC 7600, PLTMC must come from directory RUNMCNP2A also.

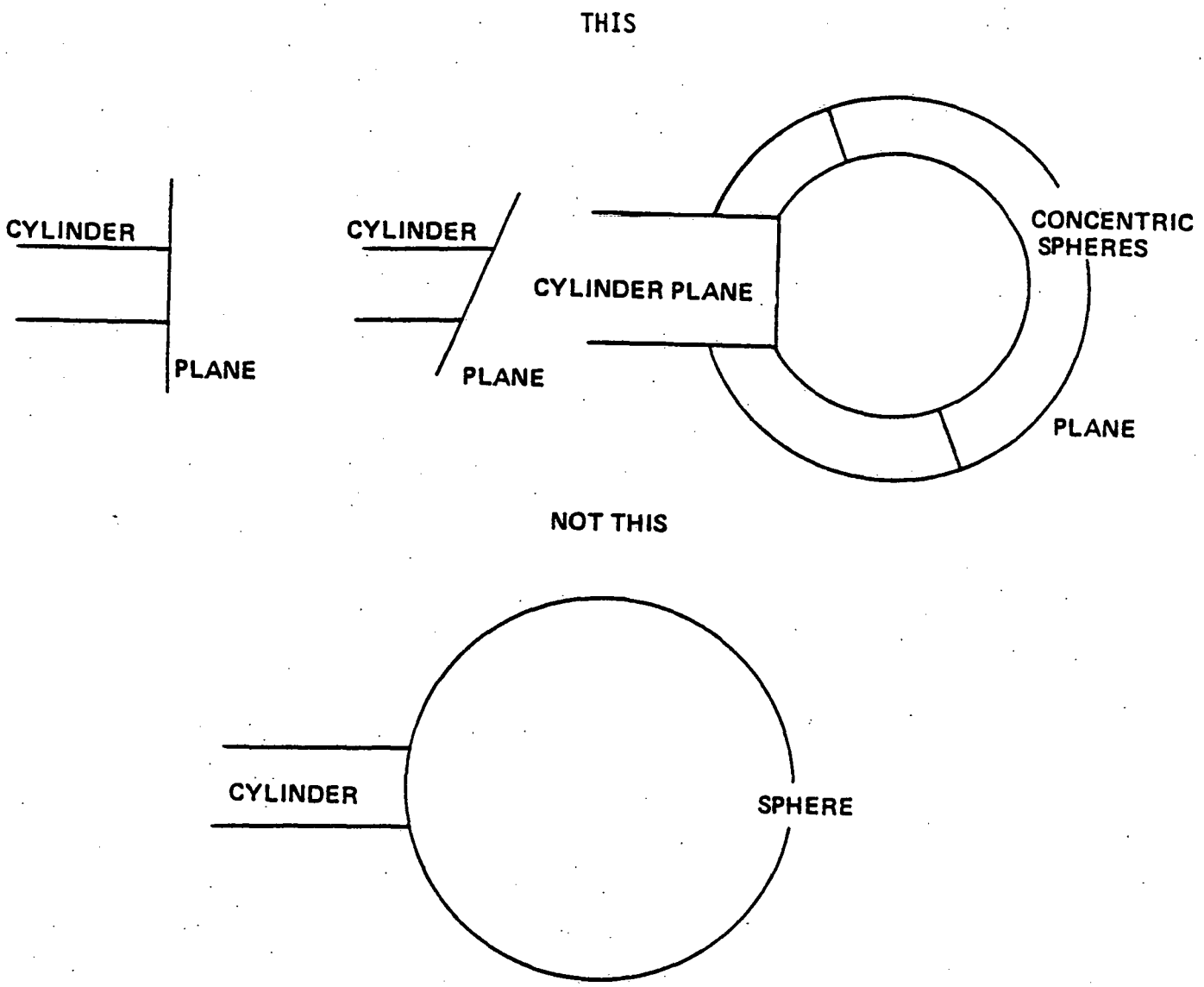

Figure B-1. Suggested MCNP Geometry Description for Cylinder Capped with a Sphere.

8) Check all ZAID numbers on material cards (p. 154) to make sure they are listed in Appendix F. Don't assume that the ZAID number for carbon, for instance, can be written as 6000. If they are not listed in Appendix F, don't use them. Use the ZAID numbers referring to the RMCCS cross section file, as this is the most up to date.

9) For ICF reactors, the tritium breeding ratio and energy deposition will not be accurate using a monoenergetic 14 MeV source. Use a homogeneous volume source in a deuterium tritium pellet of appropriate size and compression.

10) Before resorting to large run times to get neutrons to reach certain cells, consider using larger importances in the cells of interest and the cells that neutrons cross before reaching the cells of interest (see test cases W-DESI, DUMP1 for examples of this).

The following are test cases which are on the Livermore system (CDC 7600 only) for your use or modification.

DIRECTORY JSCHMO, USER #1722

MRR1	-	1 mirror case
SFRTST	-	Simplififed Univ. of Wisc. blanket
SFTST2	-	SFRTST with conical hole
SFTSTL	-	SFRTST with TBR calculation
SFTSTE	-	SFRTST with energy deposition

DIRECTORY TEMP. USER #1722

TRY2	-	2 mirror test case
UWTRY2	-	Univ. of Wisc. LD/NA system
W-DES1	-	W design for LD/NA system, W blanket, flux trap
DUMP1	-	W-DES1, with beam dump behind first mirror
E-WES1	-	W-DES1, energy deposition

TBR-W - W-DES1, TBR calculation

TMDIST - W-DES1, energy deposition with time

The next part of this appendix contains a listing of these test programs, followed by a computer plot of the geometry to scale, and in some cases, an enlargement of certain areas of the plot. Each test program is accompanied by comments which make parts of the test program easier to understand.

A LISTING OF TEST PROGRAMS AND COMPUTER PLOTS

```
spherical test problem
 1     0   -1:2                                          --------
 1  -2.0   1:1 -2:3                                     SFRTST
 2  -1.6   2:2 -3:4                                     --------
11.3 3:3 -4:5 CELL CARDS
        4:4
 1           so   600.0
 2     so  664.5
 3     so  684.5
 4     so  954.5          SURFACE CARDS
 1 1 1 1 0      STATISTICAL IMPORTANCE,NEUTRONS UNIMPORTANT ONCE
0.0 0.0 0.0 1 1.0 .5 0.0      THEY GO OUTSIDE SPHERES
14 14          ISOTROPIC POINT SOURCE
0  1
0  1
 4
n flux thru surf 4  COMMENT CARD
.000000025 .005 .02 .1 .5 1.0 2.5 5.0 7.5 10.0 15.0    ENERGY BINS
3006.01 .667 8016.01 .333
6012.01  1.0
82000.  1.0       MATERIAL CARDS
 0  15
100000
   7
```

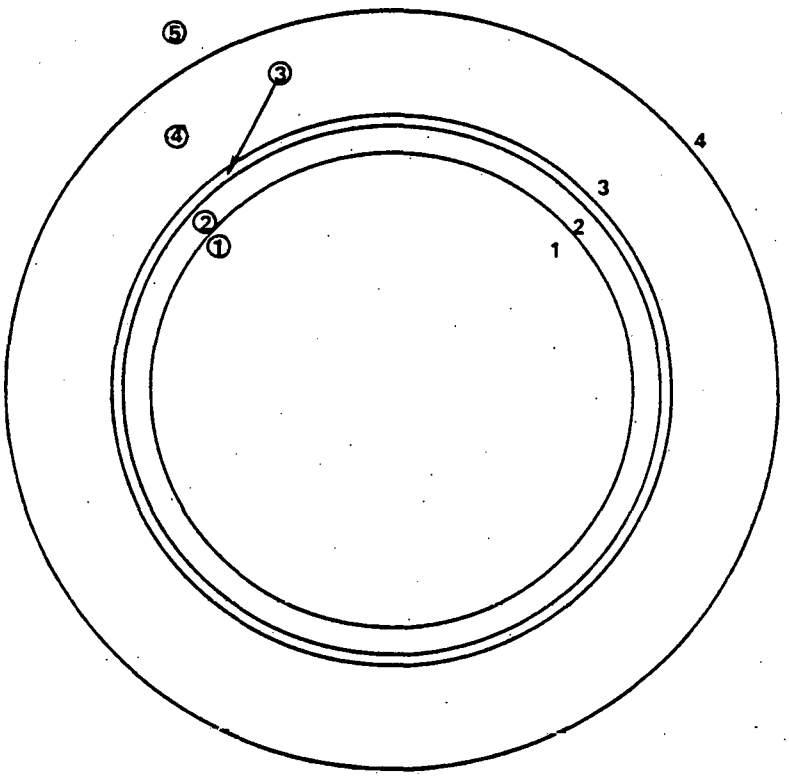

Figure B-2. Simplified SOLASE Blanket (④Cell Number, 4 Surface Number), SFRTST Geometry.

```
spherical test problem with conical hole
 1    0   -1,2,6
 2    1   -2.0    1,1 -2,3 5,6
 3    2   -1.6    2,2 -3,4 5,6
 4    3   -11.3   3,3 -4,5 5,6
 5    0      4,4,6
 6    0   1,1 -4,5  -5,2,3,4
 7
 8    1   so   600.0
 9    2   so   664.5
10    3   so   684.5
11    4   so   954.5
12     5     ky     0     .0049 1
13
14   in   1 1 1 1 0 1
15   src1 0.0 0.0 0.0 1 1.0 .5 0.0
16   sers 14 14
17  sprob 0  1
18  sbias 0  1
19   f2   4
20   fc2  n flux thru surf 4
21   e0   .000000025 .005 .02 .1 .5 1.0 2.5 5.0 7.5 10.0 15.0
22   m1   3006.01 .667 8016.01 .333
23   m2   6012.01  1.0
24   m3   82000.   1.0
25   ersn  0  15
26   nps  100000
27   ctme   7
```

SFTST2

CELL INSIDE CONE

CONICAL SURFACE

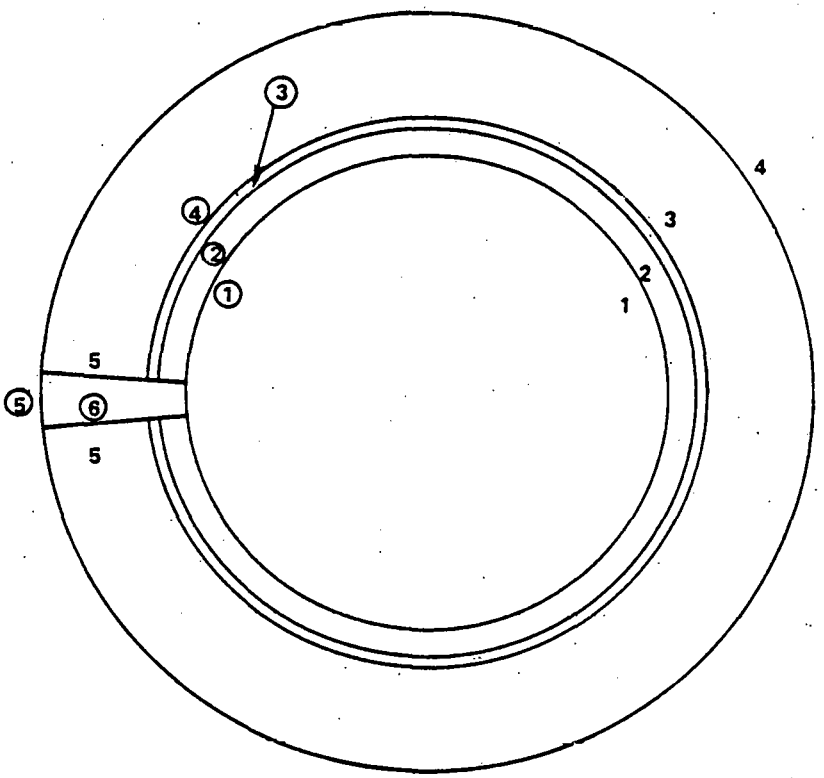

Figure B-3. Simplified SOLASE Blanket with Conical Hole, SFTST2 Geometry.

```
spherical test problem w/ computation of h3 production
 1      0   -1,2
 2    1 -2.0   1,1 -2,3
 3    2 -1.6   2,2 -3,4                                    ---------
 4    3 -11.3  3,3 -4,5    SFRTST GEOMETRY                  SFTSTL
 5    0        4,4                                        ---------
 6
 7    1     so    600.0
 8    2     so   664.5
 9    3     so   684.5
10    4     so   954.5
11
12    in    1 1 1 1 0
13    src1  0.0 0.0 0.0 1 1.0 .5 0.0
14    sers  14 14
15  sprob 0  1
16  sbias 0  1
17    f4    2
18    f24       2
19    fc4   lithium 6
20    m1    3006.10  .05 8016.04  .333   3007.05 .617
21    m2    6012.10  1.0
22    m3    82000.   1.0
23  m4      3006.10 1.0          EXTRA MATERIAL CARDS FOR
24  m5       3007.05 1.0           TALLY MULTIPLIER CARDS
25    ersn  0  15
26    nps   100000
27  ctme      7
28  e0      1e-11 4.14e-7 6.826e-7 1.855e-6 5.044e-6
29            1.371e-5 3.727e-5 1.013e-4 2.754e-4 7.485e-4 .002035 .005531
30           0.01503 .04087 .1111 .1832 .302
31           .4979 .8208 1.353 2.231 3.679 5.488 7.408 10. 12.21 13.5 14.92
32  fm64       2.41e7    5  91     TALLY MULTIPLIER CARD
33  f64          2    ↖ATOM DENSITY(LI 6) ATM/B-CM TIMES VOLUME
34  fm4   1.955e6   4  107        TALLY MULTIPLIER CARD
35  fc64      ↖lithium 7
-              ATOM DENSITY(LI 7) ,ATM/B-CM TIMES VOLUME
```

```
 1 spherical test problem w/ computation of energy deposition
 2  1      0  -1,2
 3  2     1 -2.0  1,1 -2,3
 4  3     2 -1.6  2,2 -3,4
 5  4     3 -11.3 3,3 -4,5   SFRTST GEOMETRY          --------
 6  5     0       4,4                                 SFTSTE
 7                                                    --------
 8  1     so   600.0
 9  2     so  664.5
10  3     so  684.5
11  4     so  954.5
12
13 mode    1              NEUTRON + PHOTON MODE (DEFAULT IS NEUTRON ONLY MODE)
14 ip     1 1 1 1 0
15  in    1 1 1 1 0
16  src1 0.0 0.0 0.0 1 1.0 .5 0.0
17  sers 14 14
18 sprob 0  1
19 sbias 0  1
20  m1    3006.10  .05 8016.04  .333   3007.05 .617
21  m2    6012.10  1.0
22  m3    82000.   1.0
23  ersn   0  15
24  nps   100000
25 ctme     7
26 e0     1e-11 4.14e-7 6.826e-7 1.855e-6 5.044e-6
27          1.371e-5 3.727e-5 1.013e-4 2.754e-4 7.485e-4 .002035 .005531
28         0.01503 .04087 .1111 .1832 .302
29         .4979 .8208 1.353 2.231 3.679 5.488 7.408 10. 12.21 13.5 14.92
30 f6       2
31 f16      2
32 f26      3
33 f46      4       ENERGY DEPOSITION TALLIES
34 f36      3
35 f56      4
```

```
 1 2 conc. sfrs, extended shielded cone,iron mrr,sodfrey cells
 2 1        0 -1,2,4
 3 2        1 -2.0 1,1 -2,3 4,4
 4 3        3 -11.3 2,2 -3,6,5 4,4
 5 4        0 (-7,7 : 8,7 : 6,7) -4,6,2,3  -9,8  1,1    USE OF UNION OPERATORS RATHER THAN INTERSECTION
 6 5        0 -9,8 : 3,3 : 5,6                                          OPERATORS
 7 6     3 -11.3 -5,5 -9,8 4,4 3,3                        MRR1
 8 7        2 -2.7 -6,4 7,4 -8,4                          ------
 9 8        0 9,4,5,6
10                        MIRROR IS DISK SHAPED
11 1       so 1000
12 2       so 1100
13 3       so 1200
14 4       ky 0 .0049 1
15 5       cy 400
16 6       sq 1 1 2 -2 0                  CYLINDER,      AXIS PASSES THROUGH Y AXIS  AT
17            0 6000 -6000 0 8920000      45 DEGREES  IN XY PLANE
18 7        p 1 1 0 2999
19 8        p 1 1 0 3001
20 9        py 3300
21
22 m1         3006.10 .667 8016.04 .333
23 m2         26000.11 1.0
24 m3          82000. 1.0
25 f1          7
26 fc1    n hits on iron mrr
27 in       1 1 1 1 0 1 1 0
28 src1     0 0 0 1 1 .5 0
29 sers      14 14
30 sprob     0   1
31 sbias     0   1
32 e0         2.5e-8 .005 .02 .1 .5 1 2.5 5 7.5 10 15
33 ersn     0 15
34 nps       1000000
35 ctme      7
```

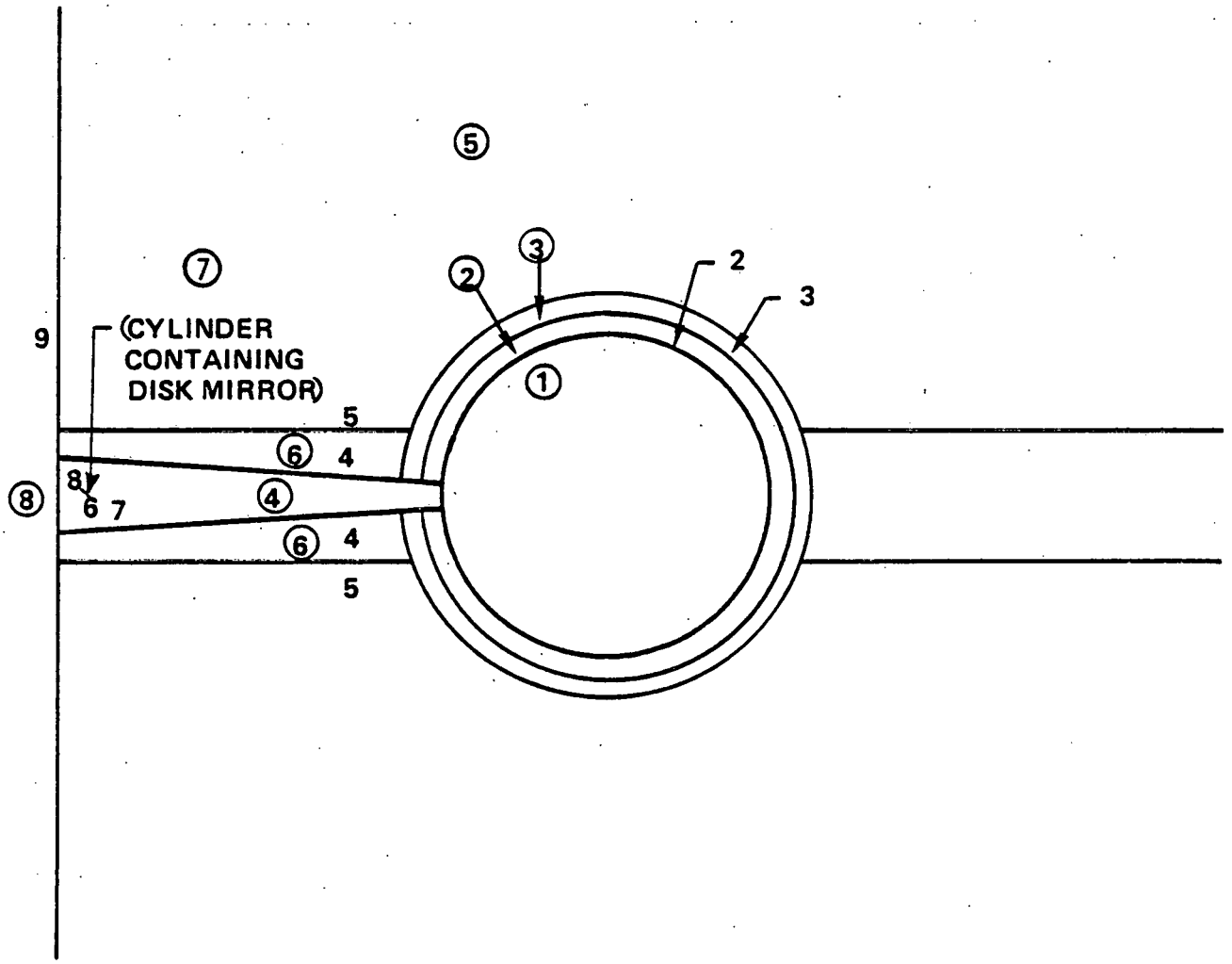

MRR 1 GEOMETRY

Figure B-4. One Mirror Case, MRR1 Geometry.

```
 1 two mirror problem
 2 1       0 -1,2,4
 3 2       1 -2.0 1,1 4,4 -2,3
 4 3       2 -1.6 2,2 4,4 -3,12
 5 4       0 1,1 -4,2,3,5   -22,6
 6 5       3 -2.5   4,4 -5,12,13  21,12 -22,6
 7 6       0 (-29,19:28,20:10,7,19,20) -6,13,17  22,4,5 23,8,14
 8 7       4 -2.7 8,19 -9,20 -10,6
 9 8       0 -11,14 -23,6 24,9
10 9       0 (17,10 : -15,10 : 16,10) -13,15,18 -24,8,14 -25,11,16
11 10      4 -2.7 15,9 -16,9 -17,9
12 11      0 25,9 -20,16 -19,12
13 12     0 19,11,16:18,16:14,15,18:12,14:7,13,17:5,5:3,3:-21,5
14 13      3 -2.5 6,6   -7,12  12,14 5,5 -26,17
15 14      3 -2.5 11,8 -23,6 24,9 -12,12,13,15
16 15      3 -2.5 13,9 -14,12 12,14 18,16 27,18
17 16      3 -2.5 25,9 -19,12 20,11 -18,12,15
18 17       3 -2.5 6,6 -7,12 26,13
19 18       3 -2.5 13,9 -14,12 -27,15
20 19         4 -2.7 29,6 -8,7 -10,6
21 20        4  -2.7 9,7 -28,6 -10,6
22
23 1       so 1000
24 2       so 1100
25 3       so 1200
26 4       ky 0 .0003 1
27 5       cy 300
28 6       sy 3000 500
29 7       sy 3000 600
30 8       p 1 1 0 2999
31 9       p 1 1 0 3001
32 10      sq 1 1 2 -2 0                    SAME CYLINDER AS IN MRR1,
33            0 6000 -6000 0 8995100          SMALLER IN RADIUS
34 11      c/x 3000 0 50
35 12      c/x 3000 0 300
36 13      s -3000 3000 0 500
37 14      s -3000 3000 0 600
38 15      p 1 1 0 -1
39 16      p 1 1 0 1
```

TRY2

```
40 17      sq 1 1 2 -2 0                          SAME CYLINDER AS ABOVE, TRANSLATED
41            0 12000 -12000 0 35995100            2000 CM IN -X DIRECTION
42 18      c/y -3000 0 300
43 19      py 4500
44 20      c/y -3000 0 50
45 21      py 1200
46 22      py 2600
47 23      px -400
48 24      px -2600
49 25      py 3400
50 28         p 1 1 0 3022.6
51 29        p 1 1 0 2977.4
52 27      p 1 1 0 0
53 26      p 1 1 0 3000
54
55 m1       3006.10 .05 3007.05 .617 8016.04 .333
56 m2       6012.10 1.0
57 m3       6012.10 .1 5000.01 .4 26000.11 .5
58 m4       13027.04 1.0
59 in        1 10r 0 1 1 1 1 1 1  1  1
60 src1     0 0 0 1 13333.3 1.0 .99985     POINT SOURCE, EMITS IN CONE    .99985 COSINE OF
61 sers     14 14                             HALF ANGLE OF CONE
62 sprob     0 1
63 sbias     0 1
64 e0       3e-8 1e-7 1e-6 1e-5 1e-4 .001 .01 .1 1.0 10.0 15.0
65 ersn     0  15
66 nps      1000000
67 ctme       5
68 f1      19
69 f21      23
70 f41      24
71 fc1     neutrons reflected twice
72 fc21     neutrons reflected once, start of column
73 fc41     neutrons reflected once, end of column
-74      cutn     1.0e123  .001  0  0     NO WEIGHT CUTOFF,ANALOG CAPTURE
                TIME      ENERGY
                           CUTOFF
                CUTOFF
```

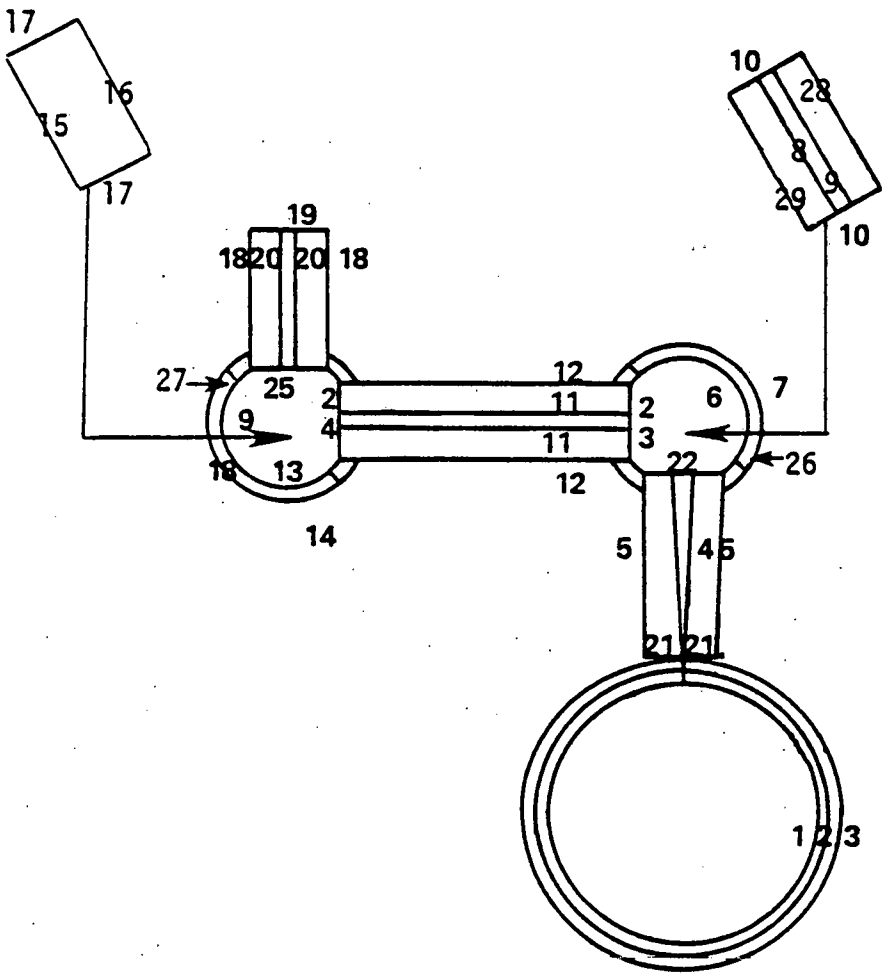

705569-24A

TRY2 GEOMETRY
SURFACES ONLY

Figure B-5. Two Mirror Test Case, TRY2 Geometry.

```
 1 uw design
 2 1        0 -1,2,5
 3 2         1 -2.0 1,1 -2,3 5,5
 4 3        2 -1.6 2,2 -3,4 5,5
 5 4       3 -2.3 3,3 -4,20 6,22 5,5
 6 5        0 1,1 -5,2,3,4,22 -8,6
 7 6        0 -7,7,23,22,19 8,5 9,9 (-24,16:19,18:28,16,17,18)
 8 7        6 -1.0 -6,20 27,19 7,6 30,23
 9 8        3 -2.3 -18,23,22 31,21  11,9 15,11 12,10 -13,20
10 9       0 -11,8,23,22 10,10 -9,6
11 10       0 -12,8,21 -10,9 -14,11 (-20,13:23,15:29,13,14,15)
12 11       0 14,10 -16,12 -15,8,20
13 12        7 -2.64 16,11 -17,24 -15,20
14 13        4 -2.36 -29,10 20,10 -21,14
15 14         5 -.083 21,13 -29,10 -22,15
16 15       4 -2.36 22,14 -23,10 -29,10
17 16      4 -2.36   24,6 -28,6 -25,17
18 17         5 -.083 25,16 -28,6 -26,18
19 18        4 -2.36 26,17 -28,6  -19,6
20 19        3 -2.3  -6,20 7,6 30,22 -27,7
21 20      0 4,4 6,7,19,22,23 13,8,21 15,11,12 -17,24
22 21        3 -2.3 -13,20 12,10 -31,8 -18,22
23 22         3 -2.3 5,5 11,9 -6,20,4 7,6 -30,19 -27,23 18,8,21
24 23         6 -1.0 27,22 18,8 11,9 7,6 -30,7 -6,20
25 24      0 17,12,20
26
27  1         so 600
28 2         so 664.5
29 3         so 684.5
30 4           so 1044.5
31 5           ky 0 .00802 1
32 6         sy 1500 465
33 7         sy 1500 200
34 8          py  1340
35 9          px -160
36 10           px -340
37 11         c/x 1500 0 120
38 12         s -500 1500 0 200
39 13         s -500 1500 0 465
40 14           py 1660
41 15          c/y -500 0 120
42 16         py 2000
```

UWTRY2

SOLASE LD/NA SYSTEM
INPUT FILE

```
43 17          py 2050
44 18         px -250
45 19        p 1 1 0 1589.8
46 20        p 1 1 0 910.2
47 21          p 1 1 0 913.8
48 22        p 1 1 0 996.4
49 23         p 1 1 0 1000
50 24         p 1 1 0 1500
51 25          p 1 1 0 1503.6
52 26            p 1 1 0 1586.2
53 27          py 1500
54 28         sq 1 1 2 -2 0
55            0 3000 -3000 0 2192200
56 29              sq 1 1 2 -2 0
57                0 4000 -4000 0 3942200
58 30       f 552.08 370 0 562049.6
59 31       f   4 3 0 2500
60
61 m1       3006.10 7.5 3007.05 92.5   8016.04  50
62 m2            6012.10 1.0
63 m3        20000.10 -.2433 8016.04 -.467 14000.02 -.2024
64             6012.10 -.0492 1001.04 -.0083
65 m4          13027.04 -.89  8016.04 -.1    1001.04 -.01
66 m5          13027.04 1.0
67 m6           13027.04 -.048 5000.01 -.009 6012.10 -.091
68              82000.10 -.382 8016.04 -.421 1001.04 -.049
69 m7          14000.02 1 8016.04  2
70 in       1 6r 7 2r 50 50 7 2r 1 3r 0 7 1 1 0     NEUTRON S ARE MULTIPLIED AS THEY REACH
71 src1     0 0 0 1 501.756 1.0 .996014                REGIONS THAT ARE MORE IMPORTANT TO THE
72 sers       14 14      CONE SOURCE                          PROBLEM
73 sprob   0  1
74 sbias  0  1
75 e0       3e-8 1e-7 1e-6 1e-5 1e-4 .001 .01 .1 1.0 10.0  15.0
76 nps      1000000
77 ctme      7
78 f1       8
79 f21      9
80 f41       10
81 f61       14
82 f81       16
83 f101      17
```

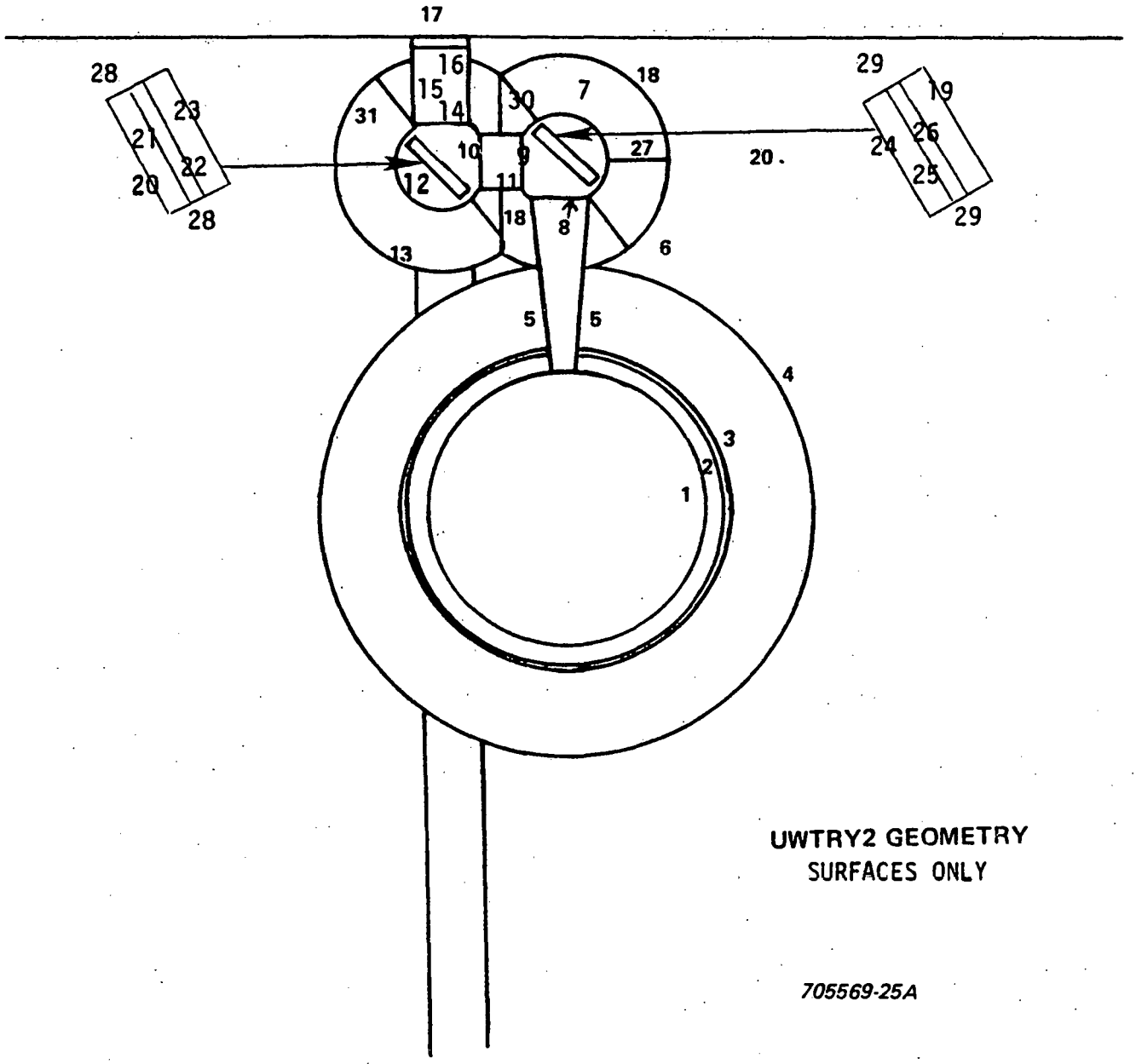

Figure B-6. SOLASE Laser Duct Neutron Attenuation System, UWTRY2 Geometry.

```
 1 westinghouse design,2 mrrs ,12 conc. sfrs
 2 1       0 -1,2,4
 3 2       1 -16.6 1,1 4,4 -2,3
 4 3       2 -.7 2,2 4,4 -3,21
 5 4       0 1,1 -4,2,3,5,21,22,23,24,25,26,27,28,29   -22,6
 6 5       8 -2.5   4,4 -5,12,13  21,12 -22,6
 7 6       0 (-29,19:28,20:10,7,19,20) -6,13,17  22,4,5 23,8,14
 8 7       9 -.083 8,19 -9,20 -10,6
 9 8       0 -11,14 -23,6 24,9
10 9       0 (17,10,30,31 : 40,31 : -39,30) -13,15,18 -24,8,14 -25,11,16
11 10      9 -.083 15,30 -16,31 -17,9
12 11      0 25,9 -20,16 -19,12
13 12     0 19,11,16:18,16:14,15,18:12,14:7,13,17:5,5:38,29:-21,5
14 13      8 -2.5 6,6   -7,12  12,14 5,5 -26,17
15 14      8 -2.5 11,8 -23,6 24,9 -12,12,13,15
16 15      8 -2.5 13,9 -14,12 12,14 18,16 27,18
17 16      8 -2.5 25,9 -19,12 20,11 -18,12,15
18 17       8 -2.5 6,6 -7,12 26,13
19 18       8 -2.5 13,9 -14,12 -27,15
20 19         9 -2.7 29,6 -8,7 -10,6
21 20        9 -2.7 9,7 -28,6 -10,6
22 21       3 -7.8 3,3 -30,22 4,4
23 22       4   -.79 -31,23 30,21 4,4
24 23      5   -2.235  31,22 -32,24 4,4
25 24      4  -.79  32,23 -33,25 4,4
26 25        3 -7.8 33,24 -34,26 4,4
27 26       6 -.1 34,25 -35,27 4,4
28 27       7 -2.6 35,26 -36,28 4,4
29 28       0 36,27 -37,29 4,4
30 29         7  -2.6 37,28 -38,12 4,4
31 30      9 -2.7 -17,9 39,9 -15,10
32 31        9 -2.7 -17,9 -40,9 16,10
```

W-DES1

WESTINGHOUSE BLANKET AND LI/NA SYSTEM WITHOUT FLUX TRAP

```
33
34 1       so 1000
35 2       so 1001
36 3       so 1013.0
37 4       ky 0 .0003 1
38 5       cy 80
39 6       sy 3000 100
40 7       sy 3000 200
41 8       p 1 1 0 3001.4
42 9       p 1 1 0 3043.8
43 10      sq 1 1 2 -2 0
44            0 6000 -6000 0 8990200
45 11      c/x 3000 0 50
46 12      c/x 3000 0 60
47 13      s -2000 3000 0 100
48 14      s -2000 3000 0 200
49 15      p 1 1 0 956.2
50 16      p 1 1 0 998.6
51 17      sq 1 1 2 -2 0
52            0 10000 -10000 0 24990200
53 18      c/y -2000 0 80
54 19      py 4500
55 20      c/y -2000 0 50
56 21      py 2198
57 22      py 2940
58 23      px -80
59 24      px -1920
60 25      py 3060
61 28         p 1 1 0 3045.2
62 29        p 1 1 0 3000
63 27      p 3 4 0 6000
64 26    p 3 4 0 12000
65 30      so 1015
66 31       so 1073
67 32         so 1093
68 33       so 1095
69 34         so 1097.5
70 35       so 1128
71 36       so 1228
72 37       so 1998
73 38       so 2198
```

```
 74 39            p 1 1 0 954.8
 75 40          p 1 1 0 1000
 76
 77 in       1 6r 25 1e3 1e3 1e4 0 1 25 1e3
 78           1e4 1 1e3 1 10r 1e3 1e3
 79 m1        73181.02  1
 80 m2         26000.11 -.328 3007.05 -.628 3006.10 -.044
 81 m3        26000.11 1.0
 82 m4          26000.11 -.397 3007.05 -.564 3006.10 -.03
 83 m5         26000.11 .104 6012.10 .896
 84 m6       8016.04 .638 14000.02 .19 13027.04 .172
 85 m7       26000.11 .035 20000.10 .0693 14000.02 .0824
 86            8016.04 .3296 6012.10 .047 1001.04 .4367
 87 m8        20000.10 -.2433 8016.04 -.467 14000.02 -.2024
 88             6012.10 -.0492 1001.04 -.0083 5000.01 -.03
 89 m9        13027.04   1.0
 90 src1     0 0 0 1 13333.3 1.0 .99985
 91 sers     14 14
 92 sprob     0 1
 93 sbias     0 1
 94 e0       3e-8 1e-7 1e-6 1e-5 1e-4 .001 .01 .1 1.0 10.0 15.0
 95 ersn     0  15
 96 nps      1000000
 97 ctme       10
 98 f1      19
 99 f21      23
100 f41      24
101 fc1      neutrons reflected twice
102 fc21      neutrons reflected once, start of column
103 fc41      neutrons reflected once, end of column
104 cutn         1.0e123  .001  0  0
```

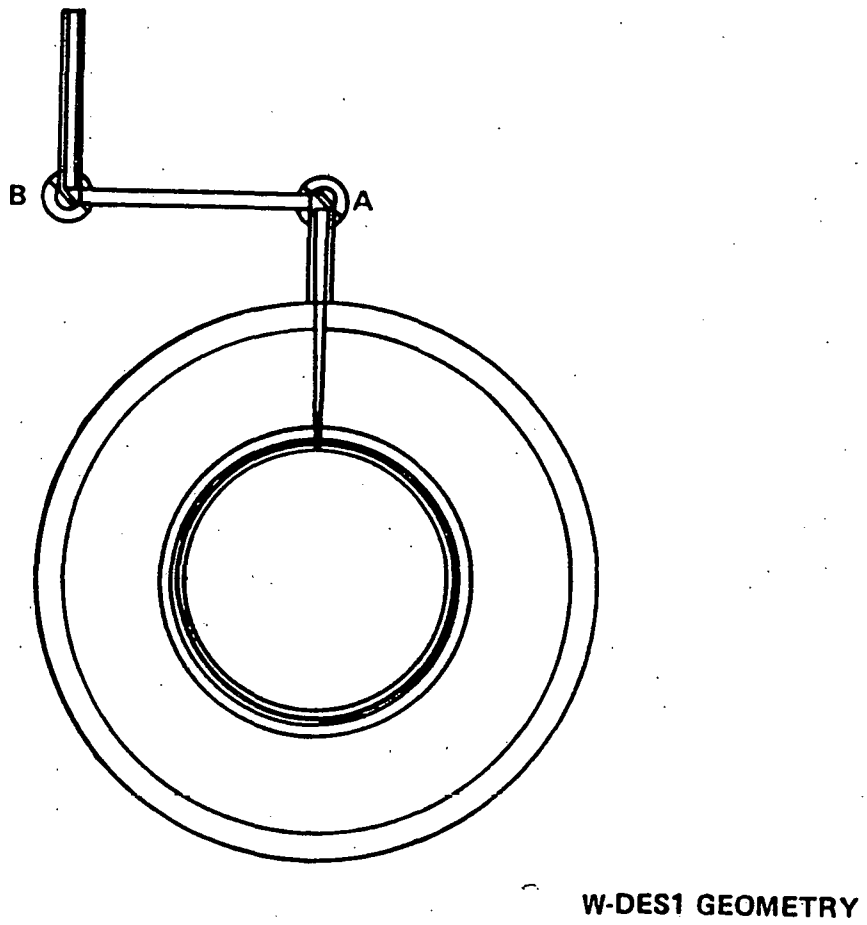

Figure B-7. Westinghouse Blanket and Laser Duct System, W-DES1 Geometry.

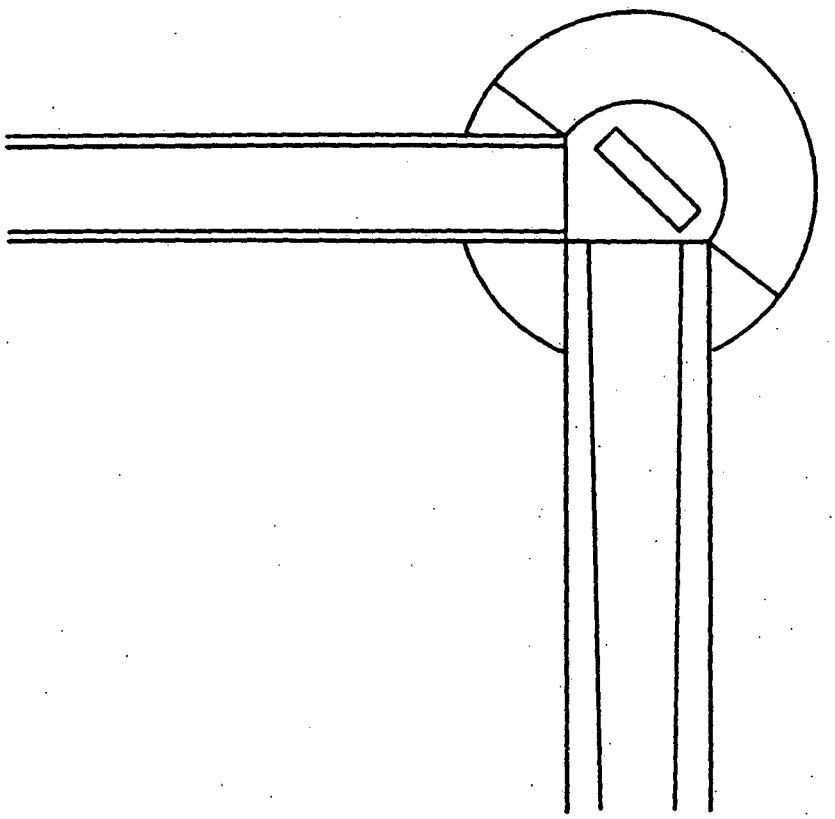

Figure B-8. Blowup of Mirror A Region in Figure B-7

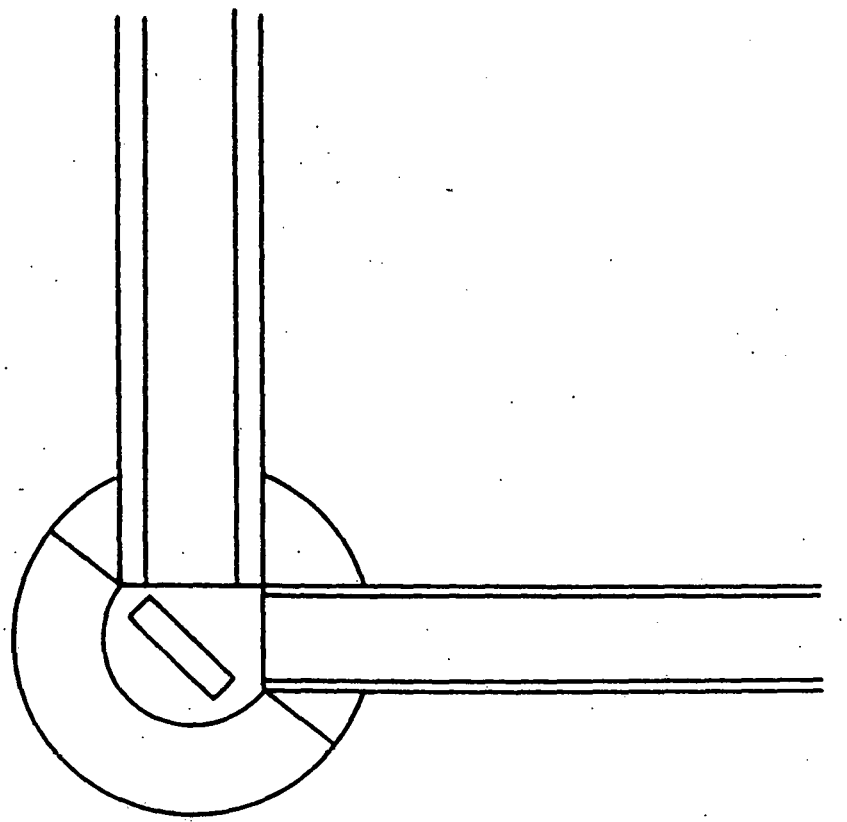

Figure B-9. Blowup of Mirror B Region in Figure B-7

```
 1 westinshouse desisn,2 mrrs ,12 conc. sfrs
 2 1       0 -1,2,4  41,32
 3 2       1 -16.6 1,1 4,4 -2,3
 4 3       2 -.7 2,2 4,4 -3,21
 5 4       0 1,1 -4,2,3,5,21,22,23,24,25,26,27,28,29   -22,6
 6 5       8 -2.5   4,4 -5,12,13  21,12 -22,6
 7 6       0 (-29,19:28,20:10,7,19,20) -6,13,17  22,4,5 23,8,14
 8 7       9 -.083 8,19 -9,20 -10,6
 9 8       0 -11,14 -23,6 24,9
10 9       0 (17,10,30,31 : 40,31 : -39,30) -13,15,18 -24,8,14 -25,11,16
11 10      9 -.083 15,30 -16,31 -17,9
12 11      0 25,9 -20,16 -19,12
13 12     0 19,11,16:18,16:14,15,18:12,14:7,13,17:5,5:38,29:-21,5
14 13      8 -2.5 6,6   -7,12  12,14 5,5 -26,17
15 14      8 -2.5 11,8 -23,6 24,9 -12,12,13,15
16 15      8 -2.5 13,9 -14,12 12,14 18,16 27,18
17 16      8 -2.5 25,9 -19,12 20,11 -18,12,15
18 17       8 -2.5 6,6 -7,12 26,13
19 18       8 -2.5 13,9 -14,12 -27,15
20 19         9 -2.7 29,6 -8,7 -10,6
21 20        9 -2.7 9,7 -28,6 -10,6
22 21       3 -7.8 3,3 -30,22 4,4
23 22       4    -.79 -31,23 30,21 4,4
24 23      5    -2.235  31,22 -32,24 4,4
25 24      4   -.79  32,23 -33,25 4,4
26 25        3 -7.8 33,24 -34,26 4,4
27 26       6 -.1 34,25 -35,27 4,4
28 27       7 -2.6 35,26 -36,28 4,4
29 28       0 36,27 -37,29 4,4
30 29         7  -2.6 37,28 -38,12 4,4
31 30      9 -2.7 -17,9 39,9 -15,10
32 31        9 -2,7 -17,9 -40,9 16,10
33 32        12 -60.0 -41,1
34
```

TBR-W

CALCULATION OF TBR FOR WESTINGHOUSE BLANKET

SAME GEOMETRY AS W-DES1 EXCEPT FOR COMPRESSED PELLET

```
35 1      so 1000
36 2      so 1001
37 3      so 1013.0
38 4      ky 0 .0003 1
39 5      cy 80
40 6      sy 3000 100
41 7      sy 3000 200
42 8      p 1 1 0 3001.4
43 9      p 1 1 0 3043.8
44 10     sq 1 1 2 -2 0
45           0 6000 -6000 0 8990200
46 11     c/x 3000 0 50
47 12     c/x 3000 0 60
48 13     s -2000 3000 0 100
49 14     s -2000 3000 0 200
50 15     p 1 1 0 956.2
51 16     p 1 1 0 998.6
52 17     sq 1 1 2 -2 0
53           0 10000 -10000 0 24990200
54 18     c/y -2000 0 80
55 19     py 4500
56 20     c/y -2000 0 50
57 21     py 2198
58 22     py 2940
59 23     px -80
60 24     px -1920
61 25     py 3060
62 28        p 1 1 0 3045.2
63 29       p 1 1 0 3000
64 27      p 3 4 0 6000
65 26     p 3 4 0 12000
66 30      so 1015
67 31       so 1073
68 32         so 1093
69 33       so 1095
70 34         so 1097.5
71 35       so 1128
72 36       so 1228
73 37       so 1998
74 38       so 2198
75 39          p 1 1 0 954.8
76 40        p 1 1 0 1000
77 41       so 0.1              SURFACE OF PELLET
78
```

```
 79 in        1 10r 0 1 18r 1
 80 m1       73181.02  1
 81 m2        26000.11 -.328 3007.05 -.628 3006.10 -.044
 82 m3       26000.11 1.0
 83 m4         26000.11 -.397 3007.05 -.564 3006.10 -.039
 84 m5        26000.11 .104 6012.10 .896
 85 m6       8016.04 .638 14000.02 .19 13027.04 .172
 86 m7       26000.11 .035 20000.10 .0693 14000.02 .0824
 87            8016.04 .3296 6012.10 .047 1001.04 .4367
 88 m8       20000.10 -.2433 8016.04 -.467 14000.02 -.2024
 89            6012.10 -.0492 1001.04 -.0083 5000.01 -.03
 90 m9       13027.04   1.0
 91 m10        3006.10 1.0
 92 m11           3007.05 1.0
 93 m12        1002.02 .5 1003.03 .5
 94 src4      0 0 0 32 1 .5 0  0.1 0     HOMOGENEOUS VOLUME SOURCE IN PELLET
 95 sers     14 14
 96 sprob     0 1
 97 sbias     0 1
 98 e0       3e-8 1e-7 1e-6 1e-5 1e-4 .001 .01 .1 1.0 10.0 15.0
 99 ersn     0  15
100 nps      1000000
101 ctme       10
102 f4        3
103 f24         3
104 f44         22
105 f64         22
106 f84            24
107 f104              24
108 fm4      4.778e5  10 107
109 fm24        5.893e6  11 91
110 fm44       2.51e6    10 107
111 fm64      3.093e7 11 91          TALLY MULTIPLIER CARDS TO CALCULATE TBR
112 fm84        9.496e4 10 107
113 fm104         1.171e6  11 91
```

```
 1 westinghouse design,2 mrrs ,12 conc. sfrs
 2 1       0 -1,2,4  41,32
 3 2       1 -16.6 1,1 4,4 -2,3
 4 3       2 -.7 2,2 4,4 -3,21
 5 4       0 1,1 -4,2,3,5,21,22,23,24,25,26,27,28,29   -22,6
 6 5       8 -2.5   4,4 -5,12,13  21,12 -22,6
 7 6       0 (-29,19:28,20:10,7,19,20) -6,13,17  22,4,5 23,8,14
 8 7       9 -.083 8,19 -9,20 -10,6
 9 8       0 -11,14 -23,6 24,9
10 9       0 (17,10,30,31 : 40,31 : -39,30) -13,15,18 -24,8,14 -25,11,16
11 10      9 -.083 15,30 -16,31 -17,9
12 11      0 25,9 -20,16 -19,12
13 12    0 19,11,16:18,16:14,15,18:12,14:7,13,17:5,5:38,29:-21,5
14 13      8 -2.5 6,6   -7,12  12,14 5,5 -26,17
15 14      8 -2.5 11,8 -23,6 24,9 -12,12,13,15
16 15      8 -2.5 13,9 -14,12 12,14 18,16 27,18
17 16      8 -2.5 25,9 -19,12 20,11 -18,12,15
18 17       8 -2.5 6,6 -7,12 26,13
19 18       8 -2.5 13,9 -14,12 -27,15
20 19         9 -2.7 29,6 -8,7 -10,6
21 20        9 -2.7 9,7 -28,6 -10,6
22 21       3 -7.8 3,3 -30,22 4,4
23 22       4   -.79 -31,23 30,21 4,4
24 23      5   -2.235  31,22 -32,24 4,4
25 24      4  -.79  32,23 -33,25 4,4
26 25        3 -7.8 33,24 -34,26 4,4
27 26       6 -.1 34,25 -35,27 4,4
28 27       7 -2.6 35,26 -36,28 4,4
29 28       0 36,27 -37,29 4,4
30 29         7  -2.6 37,28 -38,12 4,4
31 30      9 -2.7 -17,9 39,9 -15,10
32 31        9 -2.7 -17,9 -40,9 16,10
33 32        12 -60.0 -41,1
34
```

E-WES1

ENERGY DEPOSITION IN WESTINGHOUSE BLANKET
SAME GEOMETRY AS W-DES1

```
35 1      so 1000
36 2      so 1001
37 3      so 1013.0
38 4      ky 0 .0003 1
39 5      cy 80
40 6      sy 3000 100
41 7      sy 3000 200
42 8      p 1 1 0 3001.4
43 9      p 1 1 0 3043.8
44 10     sq 1 1 2 -2 0
45           0 6000 -6000 0 8990200
46 11     c/x 3000 0 50
47 12     c/x 3000 0 60
48 13     s -2000 3000 0 100
49 14     s -2000 3000 0 200
50 15     p 1 1 0 956.2
51 16     p 1 1 0 998.6
52 17     sq 1 1 2 -2 0
53           0 10000 -10000 0 24990200
54 18     c/y -2000 0 80
55 19     py 4500
56 20     c/y -2000 0 50
57 21     py 2198
58 22     py 2940
59 23     px -80
60 24     px -1920
61 25     py 3060
62 28        p 1 1 0 3045.2
63 29       p 1 1 0 3000
64 27     p 3 4 0 6000
65 26     p 3 4 0 12000
66 30       so 1015
67 31        so 1073
68 32          so 1093
69 33        so 1095
70 34          so 1097.5
71 35        so 1128
72 36        so 1228
73 37        so 1998
74 38        so 2198
75 39           p 1 1 0 954.8
76 40        p 1 1 0 1000
77 41        so 0.1
78
```

```
 79 mode   1              NEUTRON +PHOTON MODE
 80 ip       1 10r 0 1 18r 1
 81 in       1 10r 0 1 18r 1
 82 m1      73181.02  1
 83 m2       26000.11 -.328 3007.05 -.628 3006.10 -.044
 84 m3      26000.11 1.0
 85 m4        26000.11 -.397 3007.05 -.564 3006.10 -.039
 86 m5       26000.11 .104 6012.10 .896
 87 m6     8016.04 .638 14000.02 .19 13027.04 .172
 88 m7     26000.11 .035 20000.10 .0693 14000.02 .0824
 89          8016.04 .3296 6012.10 .047 1001.04 .4367
 90 m8      20000.10 -.2433 8016.04 -.467 14000.02 -.2024
 91           6012.10 -.0492 1001.04 -.0083 5000.01 -.03
 92 m9      13027.04   1.0
 93 m10       3006.10 1.0
 94 m11          3007.05 1.0
 95 m12       1002.02 .5 1003.03 .5
 96 src4     0 0 0 32 1 .5 0  0.1 0
 97 sers    14 14
 98 sprob    0 1
 99 sbias    0 1
100 e0      3e-8 1e-7 1e-6 1e-5 1e-4 .001 .01 .1 1.0 10.0 15.0
101 ersn    0  15
102 nps     1000000
103 ctme      10
104 f6      2
105 f26      3
106 f46      21
107 f66      22
108 f86      23
109 f106       24
110 f126       25
111 f146      26
112 f166       27
113 f186     29
114 f206      32
115 f16        2
116 f36        3
117 f56        21                ENERGY DEPOSITION
118 f76        22
119 f96        23
120 f116      24
121 f136       25
122 f156       26
123 f176       27
124 f196       29
125 f216        32
```

```
 1 westinghouse design,2 mrrs ,12 conc. sfrs
 2 1       0 -1,2,4  41,32
 3 2       1 -16.6 1,1 4,4 -2,3
 4 3       2 -.7 2,2 4,4 -3,21
 5 4       0 1,1 -4,2,3,5,21,22,23,24,25,26,27,28,29   -22,6
 6 5       8 -2.5   4,4 -5,12,13  21,12 -22,6
 7 6       0 (-29,19:28,20:10,7,19,20) -6,13,17  22,4,5 23,8,14
 8 7       9 -.083 8,19 -9,20 -10,6
 9 8       0 -11,14 -23,6 24,9
10 9       0 (17,10,30,31 : 40,31 : -39,30) -13,15,18 -24,8,14 -25,11,16
11 10      9 -.083 15,30 -16,31 -17,9
12 11      0 25,9 -20,16 -19,12
13 12     0 19,11,16:18,16:14,15,18:12,14:7,13,17:5,5:38,29:-21,5
14 13      8 -2.5 6,6   -7,12  12,14 5,5 -26,17
15 14      8 -2.5 11,8 -23,6 24,9 -12,12,13,15
16 15      8 -2.5 13,9 -14,12 12,14 18,16 27,18
17 16      8 -2.5 25,9 -19,12 20,11 -18,12,15
18 17       8 -2.5 6,6 -7,12 26,13
19 18       8 -2.5 13,9 -14,12 -27,15
20 19         9 -2.7 29,6 -8,7 -10,6
21 20        9 -2.7 9,7 -28,6 -10,6
22 21       3 -7.8 3,3 -30,22 4,4
23 22       4   -.79 -31,23 30,21 4,4
24 23      5   -2.235  31,22 -32,24 4,4
25 24      4  -.79  32,23 -33,25 4,4
26 25        3 -7.8 33,24 -34,26 4,4
27 26       6 -.1 34,25 -35,27 4,4
28 27       7 -2.6 35,26 -36,28 4,4
29 28       0 36,27 -37,29 4,4
30 29         7  -2.6 37,28 -38,12 4,4
31 30      9 -2.7 -17,9 39,9 -15,10
32 31        9 -2.7 -17,9 -40,9 16,10
33 32        12 -60.0 -41,1
34
35 1       so 1000
36 2       so 1001
37 3       so 1013.0
38 4       ky 0 .0003 1
39 5       cy 80
40 6       sy 3000 100
```

TMDIST

DISTRIBUTION WITH
ENR ENERGY TIME IN
WESTINGHOUSE BLANKET
SAME GEOMETRY AS W-DES1

```
41 7       sy 3000 200
42 8       p 1 1 0 3001.4
43 9       p 1 1 0 3043.8
44 10      sq 1 1 2 -2 0
45            0 6000 -6000 0 8990200
46 11      c/x 3000 0 50
47 12      c/x 3000 0 60
48 13      s -2000 3000 0 100
49 14      s -2000 3000 0 200
50 15      p 1 1 0 956.2
51 16      p 1 1 0 998.6
52 17      sq 1 1 2 -2 0
53            0 10000 -10000 0 24990200
54 18      c/y -2000 0 80
55 19      py 4500
56 20      c/y -2000 0 50
57 21      py 2198
58 22      py 2940
59 23      px -80
60 24      px -1920
61 25      py 3060
62 28         p 1 1 0 3045.2
63 29        p 1 1 0 3000
64 27      p 3 4 0 6000
65 26      p 3 4 0 12000
66 30       so 1015
67 31        so 1073
68 32          so 1093
69 33        so 1095
70 34          so 1097.5
71 35        so 1128
72 36        so 1228
73 37        so 1998
74 38        so 2198
75 39           p 1 1 0 954.8
76 40         p 1 1 0 1000
77 41        so 0.1
78
79 mode    1          NEUTRON + PHOTON MODE
80 ip        1 10r 0 1 18r 1
81 in        1 10r 0 1 18r 1
82 m1        73181.02  1
83 m2         26000.11 -.328 3007.05 -.628 3006.10 -.044
84 m3       26000.11 1.0
```

```
 85 m4          26000.11 -.397 3007.05 -.564 3006.10 -.039
 86 m5         26000.11 .104 6012.10 .896
 87 m6       8016.04 .638 14000.02 .19 13027.04 .172
 88 m7       26000.11 .035 20000.10 .0693 14000.02 .0824
 89            8016.04 .3296 6012.10 .047 1001.04 .4367
 90 m8        20000.10 -.2433 8016.04 -.467 14000.02 -.2024
 91            6012.10 -.0492 1001.04 -.0083 5000.01 -.03
 92 m9        13027.04   1.0
 93 m10         3006.10 1.0
 94 m11            3007.05 1.0
 95 m12         1002.02 .5 1003.03 .5
 96 src4       0 0 0 32 1 .5 0  0.1 0
 97 sers     14 14
 98 sprob     0 1
 99 sbias     0 1
100 ersn     0  15
101 nps      1000000
102 ctme       10
103 f6       2
104 f26       3
105 f46       21
106 f66       22
107 f86       23
108 f106        24
109 f126        25
110 f146       26
111 f166        27
112 f186      29
113 f206        32
114 f16         2
115 f36         3            ENERGY DEPOSITION
116 f56         21
117 f76         22
118 f96         23
119 f116       24
120 f136        25
121 f156        26
122 f176        27
123 f196        29
124 f216         32
125 t0     20 22 24 28 40 100 500 1000 5000 10000 50000
126          100000 500000 1000000 10000000 1.0e123          TIME BINS
```

```
 1 westinghouse design,2 mrrs ,12 conc. sfrs
 2 1       0 -1,2,4
 3 2       1 -16.6 1,1 4,4 -2,3
 4 3       2 -.7 2,2 4,4 -3,21
 5 4       0 1,1 -4,2,3,5,21,22,23,24,25,26,27,28,29   -22,6
 6 5       8 -2.5   4,4 -5,12,13  21,12 -22,6
 7 6       0 (-29,19:28,20:10,7,19,20) -6,13,17  22,4,5 23,8,14 -44,32
 8 7       9 -.083 8,19 -9,20 -10,6
 9 8       0 -11,14 -23,6 24,9
10 9       0 (17,10,30,31 : 40,31 : -39,30) -13,15,18 -24,8,14 -25,11,16
11 10      9 -.083 15,30 -16,31 -17,9
12 11      0 25,9 -20,16 -19,12
13 12    0 19,11,16:18,16:14,15,18:12,14:7,13,17:5,5:38,29:-21,5:43,33:41,33
14 13      8 -2.5 6,6   -7,12  12,14 5,5 -26,17
15 14      8 -2.5 11,8 -23,6 24,9 -12,12,13,15
16 15      8 -2.5 13,9 -14,12 12,14 18,16 27,18
17 16      8 -2.5 25,9 -19,12 20,11 -18,12,15
18 17       8 -2.5 6,6 -7,12 26,13 41,32
19 18       8 -2.5 13,9 -14,12 -27,15
20 19         9 -2.7 29,6 -8,7 -10,6
21 20        9 -2.7 9,7 -28,6 -10,6
22 21       3 -7.8 3,3 -30,22 4,4
23 22       4   -.79 -31,23 30,21 4,4
24 23      5   -2.235  31,22 -32,24 4,4
25 24      4  -.79  32,23 -33,25 4,4
26 25        3 -7.8 33,24 -34,26 4,4
27 26       6 -.1 34,25 -35,27 4,4
28 27       7 -2.6 35,26 -36,28 4,4
29 28       0 36,27 -37,29 4,4
30 29         7  -2.6 37,28 -38,12 4,4
31 30      9 -2.7 -17,9 39,9 -15,10
32 31        9 -2.7 -17,9 -40,9 16,10
33 32        0 -41,17 44,6 -42,33
34 33      8 -2.5 -41,12 -43,12 42,32
```

DUMP1

W-DES1 GEOMETRY WITH FLUX TRAP ADDED

CELLS ASSOCIATED WITH FLUX TRAP

```
35
36 1       so 1000
37 2       so 1001
38 3       so 1013.0
39 4       ky 0 .0003 1
40 5       cy 80
41 6       sy 3000 100
42 7       sy 3000 200
43 8       p 1 1 0 3001.4
44 9       p 1 1 0 3043.8
45 10      sq 1 1 2 -2 0
46            0 6000 -6000 0 8990200
47 11      c/x 3000 0 50
48 12      c/x 3000 0 60
49 13      s -2000 3000 0 100
50 14      s -2000 3000 0 200
51 15      p 1 1 0 956.2
52 16      p 1 1 0 998.6
53 17      sq 1 1 2 -2 0
54            0 10000 -10000 0 24990200
55 18      c/y -2000 0 80
56 19      py 4500
57 20      c/y -2000 0 50
58 21      py 2198
59 22      py 2940
60 23      px -80
61 24      px -1920
62 25      py 3060
63 28         p 1 1 0 3045.2
64 29         p 1 1 0 3000
65 27       p 3 4 0 6000
66 26      p 3 4 0 12000
67 30        so 1015
68 31         so 1073
69 32           so 1093
70 33         so 1095
71 34           so 1097.5
72 35          so 1128
73 36         so 1228
74 37         so 1998
75 38         so 2198
76 39            p 1 1 0 954.8
```

```
 77 40          p 1 1 0 1000
 78 41         cy 65
 79 42       py 3189.143
 80 43       py 3300
 81 44        py 3075.993
 82
 83 in        1 6r 25 1000 1000 10000 0 1 25 1000
 84          10000 -1 1000 1 10r 1000 1000 1 1
 85 m1        73181.02  1
 86 m2        26000.11 -.328 3007.05 -.628 3006.10 -.044
 87 m3        26000.11 1.0
 88 m4          26000.11 -.397 3007.05 -.564 3006.10 -.03
 89 m5        26000.11 .104 6012.10 .896
 90 m6       8016.04 .638 14000.02 .19 13027.04 .172
 91 m7       26000.11 .035 20000.10 .0693 14000.02 .0824
 92            8016.04 .3296 6012.10 .047 1001.04 .4367
 93 m8        20000.10 -.2433 8016.04 -.467 14000.02 -.2024
 94            6012.10 -.0492 1001.04 -.0083 5000.01 -.03
 95 m9        13027.04   1.0
 96 src1     0 0 0 1 13333.3 1.0 .99985
 97 sers     14 14
 98 sprob     0 1
 99 sbias     0 1
100 e0        .01 .1 1.0 10.0 15.0
101 ersn     0  15
102 nps      1000000
103 ctme       10
104 f1      19
105 f21      23
106 f41      24
107 fc1      neutrons reflected twice
108 fc21      neutrons reflected once, start of column
109 fc41      neutrons reflected once, end of column
110 cutn         1.0e123  .001  0  0
```

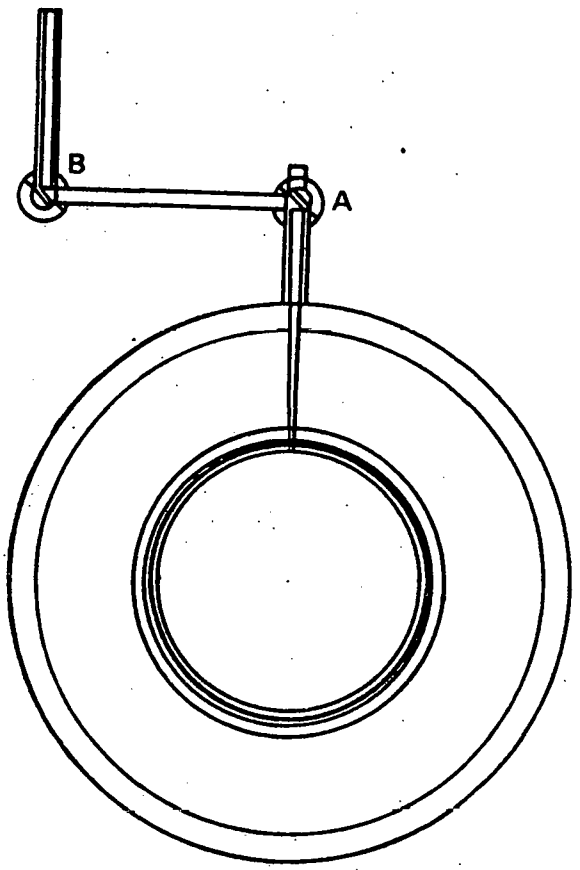

Figure B-10. Westinghouse Design with Beam Dump Behind First Mirror, DUMP1 Geometry.

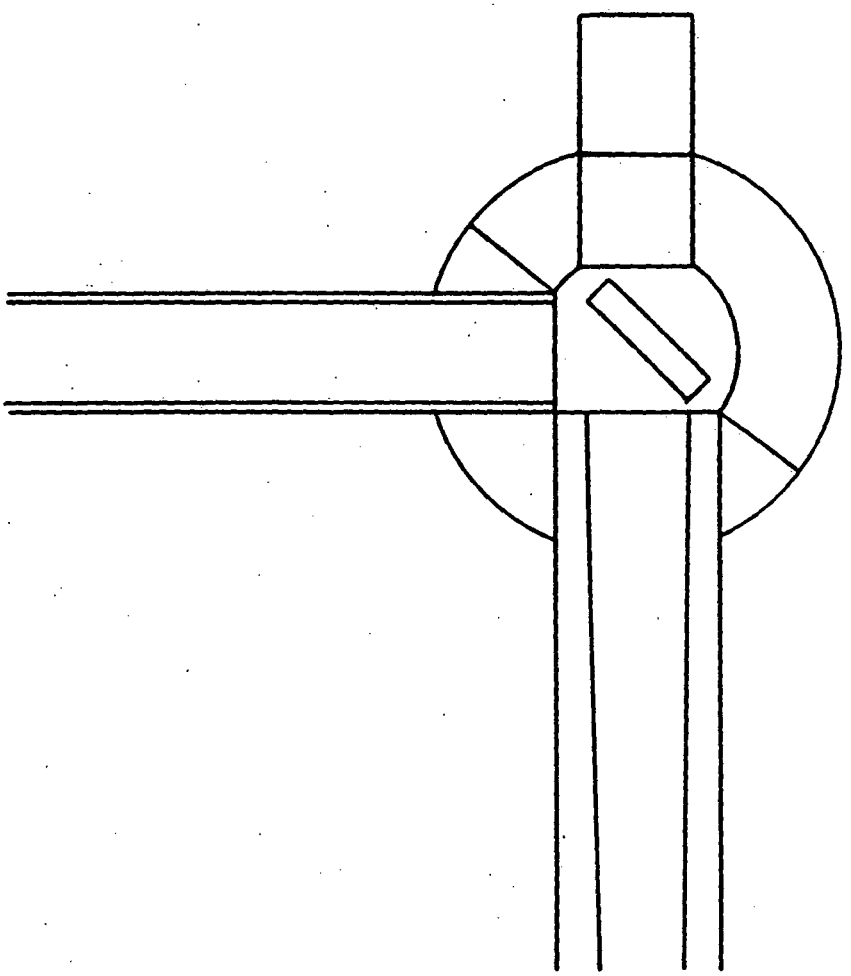

Figure B-11. Blowup of Mirror A Region in Figure B-10.

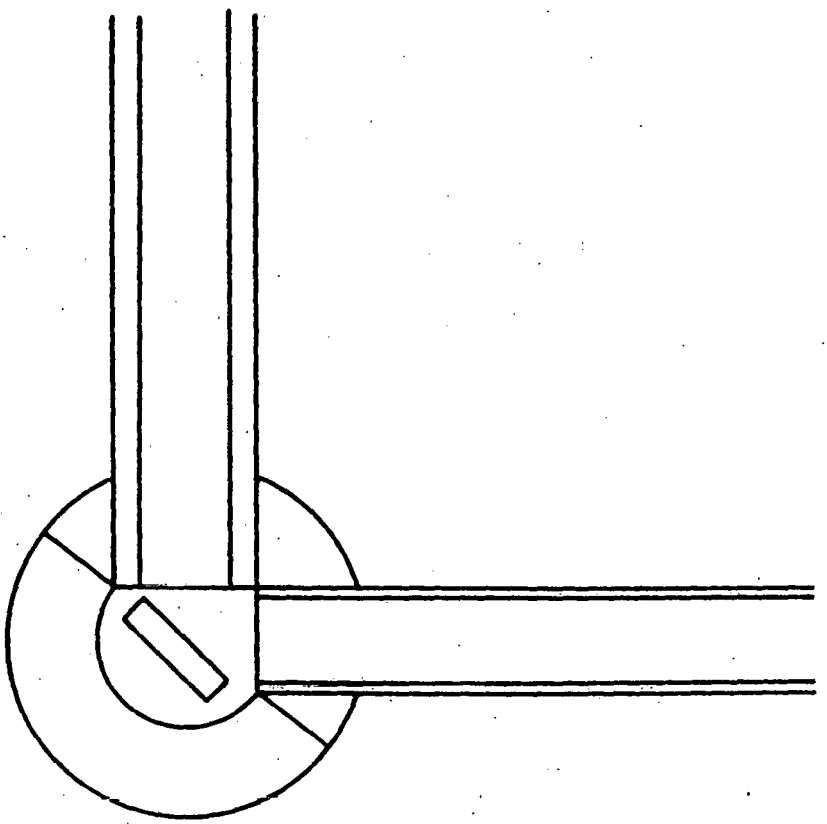

Figure B-12. Blowup of Figure B Region in Figure B-10.

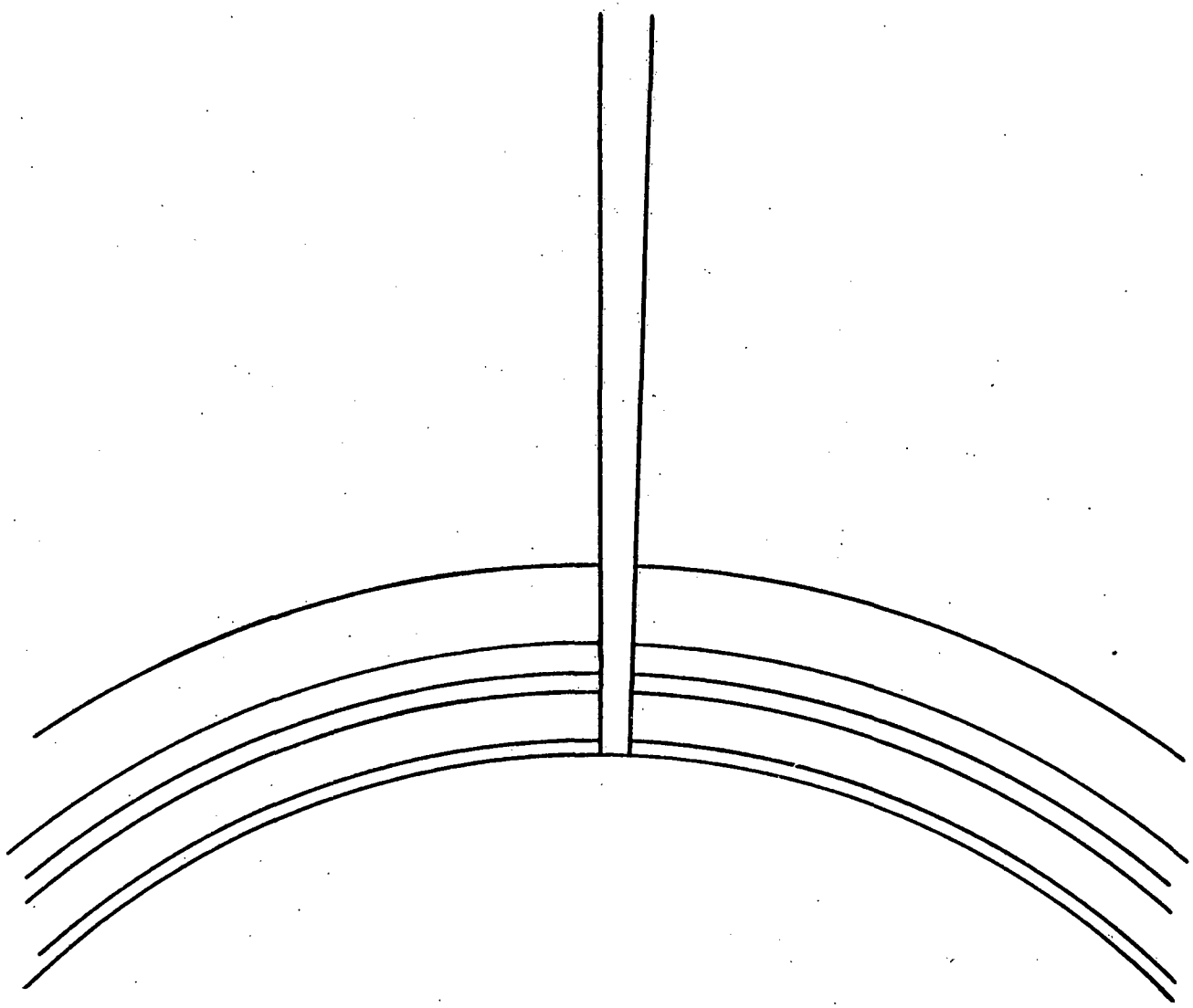

Figure B-13. Blowup of Duct Penetration in Figure B-10.